Exit from sliding in piecewise-smooth flows: deterministic vs. determinacy-breaking

Mike R. Jeffrey
Engineering Mathematics, University of Bristol, Merchant Venturer's Building, Bristol BS8 1UB, UK, email: mike.jeffrey@bristol.ac.uk
(Dated: October 9, 2015)

The collapse of flows onto hypersurfaces where their vector fields are discontinuous create highly robust states called sliding modes. The way flows *exit* from such sliding modes can lead to complex and interesting behaviour about which little is currently known. Here we examine the basic mechanisms by which a flow exits from sliding on a switching surface, or from along the intersection of two switching surfaces, with a view to understanding exit in many dimensions and with many switches. For simple sliding on a single switching surface, exit occurs via tangency of the flow to the switching surface. For sliding along an intersection of switches, exit can occur analogously at a tangency with a lower codimension sliding flow, or by a spiralling of the flow that exhibits geometric divergence (infinite steps in finite time). Determinacy-breaking can occur where a singularity creates a a set-valued flow in an otherwise deterministic system, and we resolve such dynamics as far as possible by blowing up the discontinuity into a switching layer. We show preliminary simulations exploring the role of determinacy-breaking events as organising centres of local and global dynamics.

Switching is increasingly found in dynamical models of wideranging applications, from mechanics and geophysics, to biological growth and ecology. Such systems switch between different dynamical laws whenever they encounter certain thresholds. In this paper we consider how systems behave when they exit from highly constrained states called *sliding trajectories*, which evolve along switching thresholds and intersections thereof. For one or two switches we examine the basic mechanisms of exit. In particular we show that exit from sliding is not always deterministic, and we describe main features of *determinacy-breaking* exit points. Example simulations which illustrate the theoretical results as novel dynamical phenomena are given.

I. INTRODUCTION

Many physical and biological systems are a mixture of smooth steady change and sudden transitions. A transition may occur as a *switching surface* is crossed in phase space. Perhaps surprisingly, and despite substantial progress from early local theory (see e.g. [1, 13, 28]) to recent global bifurcation theory (see e.g. [9, 10]), we are still only beginning to understand the potential effects of such switches on dynamical systems.

Consider the piecewise smooth dynamical system

$$\dot{\mathbf{x}} = \mathbf{f}(\mathbf{x};\boldsymbol{\lambda}) \ , \qquad \lambda_i = \text{sign}\left(h_i(\mathbf{x})\right) \ , \tag{1}$$

for some $i = 1, 2, ..., r$, where $\mathbf{f}$ is a vector field with smooth dependence on the variables $\mathbf{x} = (x_1, ..., x_n)$, and $\boldsymbol{\lambda} = (\lambda_1, ..., \lambda_r)$ is a vector of *switching parameters*. The dot over $\mathbf{x}$ denotes differentiation with respect to time. Each h_i is an independent scalar function, and the sets $h_i = 0$ are the *switching surfaces*.

Early piecewise-smooth models arose in electronics and mechanics, but are increasingly a feature of the life sciences and an array of other physical problems from superconductors [3] to predator-prey strategies [4, 23]. For example take the three systems

$$\ddot{x}_i = \sum_j k_{ij}(x_i - x_j) - c_i y_i - N_i \,\text{sign}(h_i) \ , \tag{2}$$

$$\dot{x}_i = \mathcal{B}\left(z_1, z_2, ..., z_n\right) - \gamma_j x_j \ , \quad z_i = \text{H}(h_i) \ , \tag{3}$$

$$\dot{x}_i = r_i x_i (1 - x_i) - \sum_{j=1}^{m} k_{ij} x_j \,\text{step}(x_i - v_i) \ , \tag{4}$$

over $i = 1, 2, ..., m$. The first represents a network of oscillators with displacements x_i, coupled via spring constants k_{ij} and damping coefficients c_i, subject to dry-friction coefficients N_i, with slipping speeds $h_i = \dot{x}_i - v$ relative to a surface with speed v. The second represents a genetic regulatory network with gene product concentrations x_i, degradation rates γ_i, and a production rate function $\mathcal{B}$ to which genes contribute if above a threshold v_i, regulated by a Hill function H [16] with argument $h_i = x_i - v_i$, often approximated as a step. The third represents a logistic growth at rate r of m populations x_i, which are consumed by other species x_j at rates k_{ij} when they exceed abundance thresholds v_i, so feeding is turned on or off by a Heaviside step function as $h_i = x_i - v_i$ changes sign, and the cannibalistic coefficients k_{ii} are usually zero. Such systems may be used to model how microscopic dry-friction leads to macroscale stick-slip or even earthquakes [2, 5], or to model networks of switching in electronic, genetic, or neural circuitry (see e.g. [14, 24]).

These are typical examples of high dimensional systems with transverse switching surfaces $h_i = 0$ for some $i = 1, 2, ..., m$, across which discontinuities occur in the differential equations. Our aim here is to show how principles learned from low dimensional discontinuous systems can be used to gain insight into such high dimensional systems. We make only preliminary steps here, studying the key features that will form the basis for future study of local and global phenomena, of which we give a few examples.

In general systems like (2)-(4) are the subject of

piecewise-smooth dynamical systems theory [9, 13, 21]. In the piecewise-smooth approach to dynamics, changes that take place abruptly at or near a threshold are modelled as discontinuities at an *event* or *switching* surface. The event surface becomes a new topological object in the qualitative theory of dynamical systems, with its own associated attractivity, singularities, and bifurcations, which comprise the growing theory of piecewise-smooth dynamical systems [6, 9].

Entry and exit points from a switching surface (see figure 1 for a few examples) are of particular interest for studying high dimensional problems, because trajectories can become constrained to one or more of the surfaces $h_i(\mathbf{x}) = 0$ as in figure 1(i), such that each exit/entry point onto a different switching surface can increase or decrease the degrees of freedom. Exit points from sliding via tangencies to a single switching surface (the second exit point in figure 1(iii)) are the only well-studied exit points so far, having been studied at the organising centres of limit cycles bifurcations in low dimensional systems [9], a study which becomes rapidly more complex in higher dimensions [15, 25].

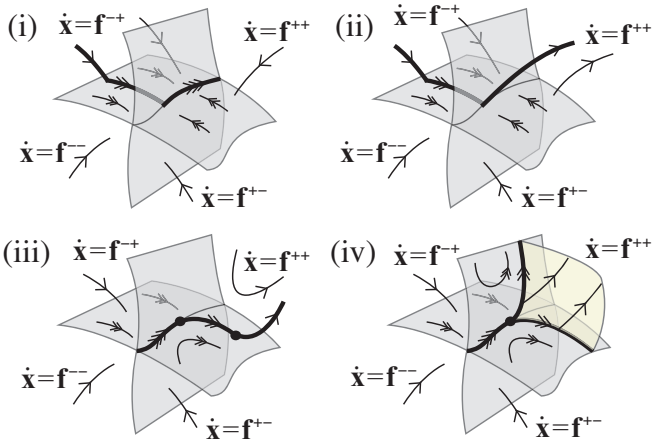

FIG. 1. Examples of: (i) entry to sliding first on a single switching surface, then the intersection of two switching surfaces, (ii) deterministic exit from codimension one sliding induced by an intersection, (ii) deterministic exit from codimension two sliding to codimension one and then to 'free' flow, both induced by tangencies, (iii) determinacy-breaking exit induced by a double tangency. The symbols $\mathbf{f}^{\pm\pm\cdots}$ denote vector fields $\mathbf{f}(\mathbf{x}; \pm 1, \pm 1, ...)$ that apply in different regions.

Exit from high codimension sliding (figure 1(iii-iv)) has so far hardly been studied, though substantial steps in this direction are starting to be made, for example in [12] where the problem of computability of solutions at exit points is raised in particular. Our aim here is to open up this problem by demonstrating basic but non-trivial behaviours induced by exit from sliding, using recent developments in piecewise smooth dynamical theory. A complete classification of exit points in general is not possible, as new topologies of exit points will appear with each higher dimension and each extra switching surface. Our aim here is instead to highlight the different forms that exit may take, and to reveal their common properties and means of study. In section V we show, for example, taking one of the model types above, how exit points in systems with multiple switches manifest as cascades between high and low order of criticality in a network of oscillators.

Ideally we should seek normal forms for the exit points we present, but there is presently no normal form theory for systems of the kind we will study, and even in the simplest nonsmooth systems, claims of normal forms and completeness of classifications have proven misleading, see [17]. We therefore seek here only to provide prototypes, or *structural models*, for the exit points currently known. It is not the precise form of the vector field expressions, but the qualitative behaviours possible and the means to study them, that concerns us here.

An important feature of exit points is whether or not they are deterministic. Determinacy-breaking (figure 1(iv)) occurs when a deterministic trajectory reaches an exit point in finite time, then generates a multi-valued flow at the exit point, with determinism still maintained elsewhere. These pose obvious conceptual problems: a numerical computation may select one of the many possible exit trajectories depending on the numerical method, while an application may require more detailed modeling to resolve the ambiguity. We shall focus only on the extent to which mathematics can resolve such points, and treat all trajectories permitted by the vector field as equally valid. Nevertheless, we shall see that in certain cases the geometry of the flow alone favours certain trajectories over others, and this is reflected in simulations.

Simulation at a determinacy-breaking point would require an event detection method, followed by a decision either to: 1) simulate an ensemble of possible onward trajectories, 2) introduce a criterion for selecting between the possible values by introducing discretisation, stochasticity, hysteresis, smoothing, or other modeling factors. The best understood of these is smoothing, or *regularization*, in which the discontinuity is replaced by a steep sigmoid transition, and for which basic results exist describing how such systems approximate discontinuous systems [22, 27]. Therefore when simulating examples of exit point behaviour for illustrative purposes only, we shall use smoothed out approximations of the discontinuous vector field as described in the text, and let the numerical integrator choose the path through the intersection as a numerical experiment. Specifically we use Mathematica's NDSolve, which for sufficiently high precision and accuracy goals yields repeatable results, and approximate sign x_i by a smooth sigmoid function $\phi(x_i/\varepsilon)$ such that $\phi(x_i/\varepsilon) \to \text{sign } x_i$ as $\varepsilon \to 0$.

We begin by setting out some preliminaries of piecewise-smooth systems in section II. We then begin our study of exit points. Exit from codimension one sliding is discussed in section III, briefly reviewing exit via tangencies, then discussing the familiar phenomenon of

exit induced by intersections. In section IV we begin the study of exit from higher codimension sliding.

Exit from sliding on an intersection of multiple switches can take place via simple tangencies as in section IV A, via multiple tangencies whose study we instigate in section IV B, or via Zeno process as in section IV C. The latter involves a flow which spirals in towards an intersection, travels along it, and spirals back out, with a determinacy-breaking event in the middle. In each case we defining a structural model for the scenario, examine its dynamics in the switching layer, and conclude with illustrative simulations. Some closing remarks are made in section VI.

II. PRELIMINARIES: RESOLVING THE DISCONTINUITY

Taking the system (1), let us assume that all of the gradient vectors ∇h_j are linearly independent. Then the manifolds $h_j = 0$ are transversal, so the number of regions N and number of switching surfaces m is related by $N = 2^m$ (assuming the number of spatial dimensions is $n \geq m$). The full switching surface is the zero set of the scalar function

$$h(\mathbf{x}) = h_1(\mathbf{x})h_2(\mathbf{x})...h_m(\mathbf{x}) \ ,$$

of which each set $h_j(\mathbf{x}) = 0$ is a submanifold. Each of the $\mathbf{f}^i$'s is a vector field that is smooth on an open region that extends across the local domain boundaries defined by the switching surface.

Throughout this paper we will use the following coordinates. At a point p where $r \leq m$ switching surfaces intersect, say the set where $h_1 = h_2 = ... = h_r = 0$ without loss of generality, we can find coordinates $\mathbf{x} = (x_1, x_2, ..., x_n)$ such that $x_i = h_i$ for $i = 1, 2, ..., r$. The switching surface in the neighbourhood of p consists of the hypersurfaces $x_1 = 0$, $x_2 = 0$, ..., $x_r = 0$, and their intersection is the set $x_1 = x_2 = ... = x_r = 0$. Vector field components are written as $\mathbf{f} = (f_1, f_2, ..., f_n)$.

The system (1) gives a well defined dynamical system in each region outside the switching surface (for $h \neq 0$), but not on the switching surface $h = 0$. The next step is therefore to prescribe the dynamics on $h = 0$.

A. Vector field combination at the discontinuity

The system (1) is typically (see e.g. [13, 18]) extended across the discontinuity by letting

$$\dot{\mathbf{x}} = \mathbf{f}\left(\mathbf{x}; \boldsymbol{\lambda}\right) \quad : \quad \begin{cases} \lambda_j = \text{sign}\left(h_j\right) & \text{if} \quad h_j \neq 0 \ , \\ \lambda_j \in [-1, +1] & \text{if} \quad h_j = 0 \ , \end{cases} \tag{5}$$

forming a differential inclusion which interpolates between the different values $\mathbf{f}$ can take in the neighbourhood of the discontinuity. You can do a lot with such a general statement, at least Filippov could, beginning with the rather important proof that solutions to the discontinuous system do exist [13]. What those solutions look like, however, and how they behave, is still an active and very open field of research.

The set-valued vector field in (5) contains vector field values that are dynamically irrelevant in the sense that the flow cannot follow them for any non-vanishing interval of time. Those values the flow *can* follow may be found by re-writing the vector in a *canopy* combination [18] of the $\mathbf{f}$'s,

$$\mathbf{f}\left(\mathbf{x}; \boldsymbol{\lambda}\right) = \sum_{i_1, i_2, ... i_m = \pm} \lambda_1^{(i_1)} \lambda_2^{(i_2)} ... \lambda_m^{(i_m)} \mathbf{f}^{i_1 i_2 ... i_m}\left(\mathbf{x}\right) \ , \quad \text{where} \quad \lambda_j^{(\pm)} \equiv (1 \pm \lambda_j)/2 \ , \tag{6}$$

using hereon the more convenient index notation

$$\mathbf{f}^{i_1 i_2 ... i_m}\left(\mathbf{x}\right) \equiv \mathbf{f}\left(\mathbf{x}; i_1 1, i_2 1, ..., i_m 1\right) \tag{7}$$

with each i_j taking either a $+$ or $-$ sign corresponding to the sign of h_j. For two switching manifolds ($m = 2$), the combination (6) becomes (omitting arguments)

$$\mathbf{f} = \frac{1+\lambda_2}{2}\left[\frac{1+\lambda_1}{2}\mathbf{f}^{++} + \frac{1-\lambda_1}{2}\mathbf{f}^{-+}\right] + \frac{1-\lambda_2}{2}\left[\frac{1+\lambda_1}{2}\mathbf{f}^{+-} + \frac{1-\lambda_1}{2}\mathbf{f}^{--}\right] \ , \tag{8}$$

and for a single switching surface ($m = 1$) this reduces to Filippov's commonly used convex combination

$$\mathbf{f}\left(\mathbf{x}\right) = \frac{1+\lambda_1}{2}\mathbf{f}^{+}\left(\mathbf{x}\right) + \frac{1-\lambda_1}{2}\mathbf{f}^{-}\left(\mathbf{x}\right) \ . \tag{9}$$

In this case the Filippov/Utkin [13, 29] criteria may be used to determine the existence of sliding modes on $h_1 = 0$. More generally to find $\boldsymbol{\lambda}$ and any possible sliding modes on the thresholds $h_j = 0$ we need the switching layer methods outlined as follows.

B. Switching layer and sliding

To reveal the dynamics hidden in the discontinuity, we follow [19] and blow up each manifold $h_j = 0$ to study the dynamics on λ_j that transports the flow across the discontinuity. We review the main points from [19, 20] here. The dynamics on each λ_j is induced by the h_i component of the flow, and thus given by

$$\lambda_j' = \mathbf{f}(\mathbf{x}; \boldsymbol{\lambda}) \cdot \nabla h_j\left(\mathbf{x}\right) \qquad \text{on} \quad h_j = 0 \ , \tag{10}$$

where the prime denotes differentiation with respect to a dummy instantaneous timescale. One way to describe this is that $\dot{x}$ denotes $\frac{d}{dt}x$ while λ' denotes $\varepsilon\frac{d}{dt}\lambda$ for infinitesimal $\varepsilon > 0$, and this particular interpretation permits singular perturbation analysis, see e.g. [20]. Each switching surface $x_i = 0$ becomes a switching layer $\{x_i = 0, \ \ \lambda_i \in [-1, +1]\}$.

At a point where $r \leq m$ switching surfaces intersect, say where $h_1 = h_2 = ... = h_r = 0$ and $h_{i>r} \neq 0$, in local coordinates $\mathbf{x} = (x_1, x_2, ..., x_n)$ where each $h_i = 0$ coincides with a coordinate level set $x_i = 0$ for $i = 1, 2, ..., r$, we then have the dynamics in the switching layer

$$\left\{ \begin{array}{rcl} (\lambda_1', ..., \lambda_r') & = & (f_1(\mathbf{x}; \boldsymbol{\lambda}) \quad , ..., f_r(\mathbf{x}; \boldsymbol{\lambda})) \ , \\ (\dot{x}_{r+1}, ..., \dot{x}_n) & = & (f_{r+1}(\mathbf{x}; \boldsymbol{\lambda}), ..., f_n(\mathbf{x}; \boldsymbol{\lambda})) \ . \end{array} \right. \tag{11}$$

If the fast λ_j' subsystem has equilibria where $\lambda_i' = 0$ for all $i = 1, ..., r$, the resulting equations

$$\left\{ \begin{array}{rcl} (0, ..., 0) & = & (f_1(\mathbf{x}; \boldsymbol{\lambda}) \quad , ..., f_r(\mathbf{x}; \boldsymbol{\lambda})) \ , \\ (\dot{x}_{r+1}, ..., \dot{x}_n) & = & (f_{r+1}(\mathbf{x}; \boldsymbol{\lambda}), ..., f_n(\mathbf{x}; \boldsymbol{\lambda})) \ , \end{array} \right. \tag{12}$$

describe states that evolve inside the switching surfaces $x_1 = ... = x_r = 0$ on the main timescale, because $\lambda_j' = 0$ implies $\dot{x}_j = \mathbf{f} \cdot \nabla h_j = 0$. These are *sliding modes* (an extension of Filippov's sliding modes [13, 18]), and the values of the λ_j's corresponding to sliding modes are thus given by

$$\mathcal{S}(\boldsymbol{\lambda}) := \left\{ \begin{array}{l} (\lambda_1, ..., \lambda_r) \in [-1, +1]^r \ : x_j = 0 \\ \ \ \& \ f_j(\mathbf{x}; \boldsymbol{\lambda}) = 0 \ \text{ for } \ j = 1, ..., r \end{array} \right\} \ . \tag{13}$$

In the absence of sliding modes, when there exist no solutions to (13) for each $\lambda_j \in [-1, +1]$, the system (11) facilitates an instantaneous transition from one boundary of $\lambda_j \in [-1, +1]$ to another, and the flow crosses through the switching surface.

When solutions $(\lambda_1, .., \lambda_r) = \mathcal{S}(\lambda_1, .., \lambda_r)$ do exist, they form invariant manifolds of the switching layer system (11), given by

$$\mathcal{M}^S = \left\{ \begin{array}{l} (\lambda_1, ..., \lambda_r) \in [-1, +1]^r \\ (x_{r+1}, ..., x_n) \in \mathbb{R}^{n-r} \end{array} \ : \ \boldsymbol{\lambda} = \mathcal{S}(\boldsymbol{\lambda}) \right\} \tag{14}$$

on which the system obeys the sliding dynamics (12). We call $\mathcal{M}^S$ the *sliding manifold*. Examples are illustrated in figure 2 for one or two switches. If it exists, $\mathcal{M}^S$ may be comprised of many connected or disconnected branches on which the conditions (14) hold, and on which $\mathcal{M}^S$ is normally hyperbolic, i.e. satisfies

$$\det \left| \frac{\partial(\lambda_1', ..., \lambda_r')}{\partial(\lambda_1, ..., \lambda_r)} \right|_{\mathcal{M}^S} \neq 0 \ . \tag{15}$$

Provided (14) and (15) hold then the manifold $\mathcal{M}^S$ so defined is invariant except at its boundaries.

The boundaries of $\mathcal{M}^S$ are points where (14) or (15) break down, which respectively give rise to:

1. *end points*: where $\mathcal{M}^S$ passes through the boundary of $\lambda_i \in [-1, +1]$ for some $i \in \{1, .., r\}$; or

2. *turning points*: where two branches of $\mathcal{M}^S$ meet (in a fold or higher catastrophe) and normal hyperbolicity of $\mathcal{M}^S$ is lost.

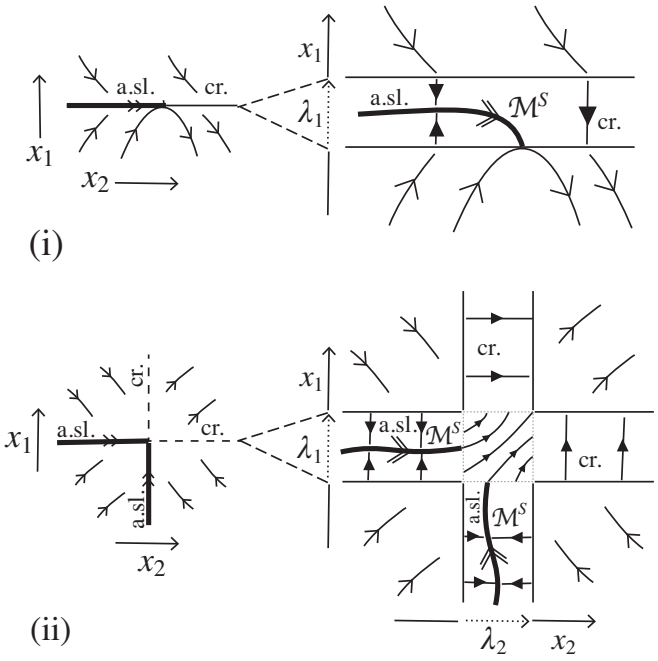

FIG. 2. Sketch showing the blow up of the switching surface into a switching layer at simples exit points. In (i) we see a crossing region (cr.), and an attracting sliding region (a.sl.) inside which an invariant manifold $\mathcal{M}^S$ exists. In (ii) we see an intersection of two switching surfaces where crossing and attracting sliding occurs over two sections of the switching surface each. In each figure the inset top-left shows the piecewise-smooth flow in the (x_1, x_2) plane, the main figure shows the switching layer where $x_j = 0$ blows up into $\lambda_j \in [-1, +1]$, with sliding on $\mathcal{M}^S$. The flow outside the switching surface is indicated with single arrows, the sliding flow on $\mathcal{M}^S$ indicated with double arrows, and the fast flow is indicated with filled arrows.

If trajectories exit from sliding they will typically do so at boundaries of $\mathcal{M}^s$ given, therefore, by these conditions. Examples of type 1 are illustrated in figure 2 for one or two switches.

In both cases 1 and 2 above, the number of roots $\mathcal{S}(\lambda)$ changes, typically by unity in the former case, because one root leaves the domain of existence, and by two in the latter case because pairs of solutions undergo fold bifurcations (for more details see [19]). We shall see interplay between these two kinds of bounds in the following sections.

An orbit is a piecewise-smooth continuous curve, along which the direction of time is preserved, formed by concatenating: solution trajectories of (5) outside the switching surface, with solution trajectories of (11) inside the switching layer. The latter are themselves concatenations of 'fast' solutions of (10), which either cross through the switching layer or collapse on to a sliding manifold $\mathcal{M}^S$, with sliding solutions of (12). (In figure 3 such concatenated trajectories are seen, but the fast solutions are not shown. In figure 2 only individual trajectories, including the fast switching layer solutions (filled arrows)

are shown to illustrate the phase portrait).

With orbits so defined, multiple orbits may be possible through a single point. In an attractive sliding region, every point has a family of distinct orbits reach it in finite time. The converse is also possible, and if a family of distinct orbits depart from a point in finite time we say the orbit is set-valued in forward time. If an orbit becomes set-valued in forward time at a specific point, we say that determinacy has been broken at that point.

III. EXIT FROM CODIMENSION $r = 1$ SLIDING

We begin by considering how orbits may exit from sliding along a codimension one switching surface $h_j = 0$.

We shall not consider points inside repelling sliding regions, occurring where $\mathbf{f}^+ \cdot \nabla h_j(\mathbf{x}) > 0$ and $\mathbf{f}^- \cdot \nabla h_j(\mathbf{x}) < 0$ on $h_j(\mathbf{x}) = 0$. The flow can exit from the switching surface at all such points, so they do not directly give rise to interesting dynamics. Moreover these are only the reverse time equivalent of attracting sliding regions, which have been well studied.

Our interest henceforth will be how trajectories are able to exit from regions of attracting sliding, which, since attractive regions are invariants of the flow (given by $\mathcal{M}^S$), can only happen at their boundaries.

A key feature of exit is whether it is deterministic or determinacy-breaking. In a deterministic exit there is only one possible trajectory that an orbit can follow through the exit point, and the two basic forms that we will discuss in the following sections are shown in figure 3 (i) and (iii), where exit occurs at a tangency (type 1 – endpoint) in (i) or at an intersection (type 2 – endpoint) with a second switching manifold in (ii). In a determinacy-breaking exit multiple trajectories may be followed beyond the exit point, and the two basic forms we will discuss are triggered by a double tangency as shown in figure 3(ii), or again by an intersection as shown in figure 3(iv); the inset in each figure illustrated the set-valued orbit through an exit point. These will be described in more detail throughout this section.

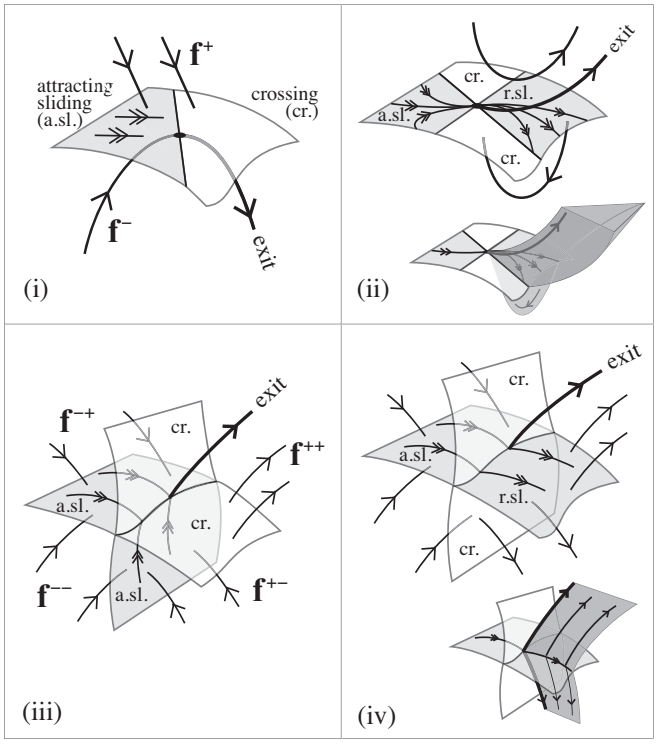

FIG. 3. Exit from codimension one sliding via: (i) a simple tangency; (ii) a two-fold singularity; (iii-iv) a double-switch. The switching surface is made up of regions where the flow is attracted to the surface then slides (a.sl.), slides but is repelled from the surface (r.sl.), or crosses (cr.). The phase portraits indicate that in (ii) and (iv) determinacy is broken at the exit point (the resulting set-valued flow is shown inset).

A. Exit via a tangency: deterministic

The simplest kind of exit point is that represented by figure 3(i), namely a simple boundary between crossing and sliding involving only a single switching manifold. Considering (13) for $r = 1$, we see that an end point of $\mathcal{M}^S$ occurs when $f_1(\mathbf{x}; \lambda_1) = 0$ is satisfied at the boundary of the switching layer, $\lambda_1 = +1$ or $\lambda_1 = -1$. Hence $f_1^{\pm}(\mathbf{x}; \pm 1) \equiv f_1^{\pm}(\mathbf{x}) = 0$, which defines a tangency between the respective vector field $\mathbf{f}^{\pm}$ and the switching manifold $h_1(\mathbf{x}) = 0$.

If the flow curves away from the switching surface at such a tangency then the flow can exit from sustained sliding at that point, and we call it a *visible* tangency. A generic visible tangency is defined as a point satisfying the conditions

$$0 = f_1^+ < \frac{d}{dt} f_1^+ \qquad \text{or} \qquad 0 = f_1^- < \frac{d}{dt} f_1^- \tag{16}$$

for a tangency of one flow (+) or the other (−).

The righthand sides of the switching layer system (11), the sliding system (12), and the discontinuous system (1), are equal precisely at points where $\mathcal{S}(\lambda_1) = +1$ or $\mathcal{S}(\lambda_1) = -1$. The dynamics at a non-degenerate tangency, i.e. a quadratic tangency of one flow only, where only one set of the conditions (16) hold, is therefore locally very simple. The flow actually transitions differentiably from sliding on the switching surface into smooth motion outside it, and by implication, such a flow is deterministic.

Simple tangencies have been well studied. They are interesting for their role in global dynamics, as the instigators of so-called *sliding bifurcations* (see [9]), whereby limit cycles or stable/unstable manifolds lose or gain connections to the switching surface. They will be of no further interest here.

A point where $\mathcal{S}(\lambda_1) = +1$ and $\mathcal{S}(\lambda_1) = -1$ are both solutions of (13), is nontrivial since (12) is then singular, and this is covered in the next section.

B. Exit via a two-fold singularity

In a system with one switching manifold, exit from sliding can happen where $\mathcal{S}(\lambda_1) = +1$ and $\mathcal{S}(\lambda_1) = -1$ are simultaneously solutions of (13). This constitutes a compound tangency as in figure 3(ii), when both vector fields are tangent to the switching surface. The flow through these compound tangencies can be set-valued in forward (as well as backward) time, which breaks the determinacy of the flow at the double tangency point itself. The simplest example of such determinacy-breaking exit via a compound tangency is the two-fold singularity, illustrated in figure 3(ii).

A tangency of either vector field can be described as a *fold* of the flow with respect to the switching surface if it is non-degenerate (if $\partial f_1^{\pm}/\partial x_1 \neq 0$ where $f_1^{\pm} = 0$, as for the simple tangency in the previous section). A double-tangency point where both $f_1^{\pm}$ vanish can be described as a *two-fold* if it is non-degenerate, meaning that certain genericity conditions are satisfied, namely that $\partial f_1^{\pm}/\partial x_1$ do not vanish locally, and that the vectors ∇x_1, $\nabla(\partial f_1^{+}/\partial x_1)$, $\nabla(\partial f_1^{-}/\partial x_1)$, are linearly independent.

The canonical form of the two-fold singularity (see [7, 13, 26]) under these conditions is

$$(\dot{x}_1, \dot{x}_2, \dot{x}_3) = \begin{cases} \mathbf{f}^+ = (-x_2, a_1, b_1) & \text{if} \quad x_1 > 0 \,, \\ \mathbf{f}^- = (+x_3, b_2, a_2) & \text{if} \quad x_1 < 0 \,, \end{cases} \tag{17}$$

in terms of constants $b_i \in \mathbb{R}$ and $a_i = \pm 1$. The singularity lies at $x_1 = x_2 = x_3 = 0$, and three dimensions are sufficient for a local analysis. The regions $x_2, x_3 > 0$ and $x_2, x_3 < 0$ on the switching surface are attracting and repelling sliding regions, respectively. There is a fold along $x_1 = x_2 = 0$, which is visible if $a_1 < 0$ (since then $\ddot{x}_1 = -a_1 > 0$), and a fold along $x_1 = x_3 = 0$, which is visible if $a_2 < 0$ (since then $\ddot{x}_1 = a_2 < 0$). To study exit points we are therefore interested in the case where one or both of a_1 and a_2 are negative.

The dynamics of (17) have been thoroughly studied (see [7] and references therein), we include it for completeness but shall review only the pertinent features here.

Different values of $b_{1,2}$ give topologically different phase portraits. The cases which create exit points are those in which the flow from the attractive sliding region traverses the singularity in finite time into the repelling sliding region. In all such cases the flow can follow an infinite number of forward trajectories resulting in determinacy-breaking as shown in figure 4 (see [7]); the relevant parameter regimes are listed in the caption.

Filippov's convex combination, given by applying (9) to (17), is

$$\begin{aligned} (\dot{x}_1, \dot{x}_2, \dot{x}_3) &= \tfrac{1+\lambda_1}{2}(-x_2, a_1, b_1) + \tfrac{1-\lambda_1}{2}(x_3, b_2, a_2) \\ &:= (F_1, F_2, F_3) \,, \end{aligned}$$

however this was shown in [20] to be structurally unstable inside the switching layer (as we show below). To obtain

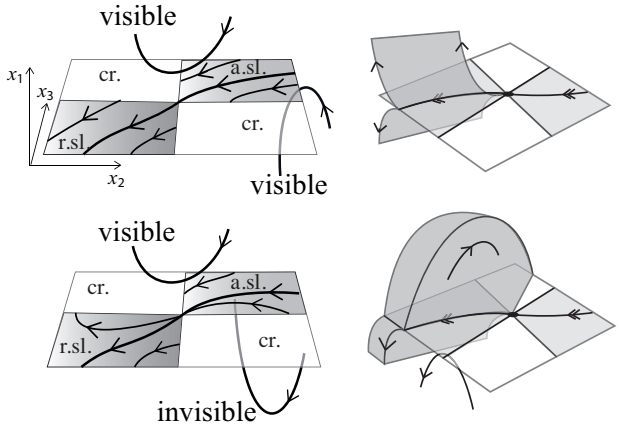

FIG. 4. Determinacy breaking in three different kinds of two-fold. Left figures sketch the piecewise-smooth flow and sliding flow, right figures show a single trajectory exploding into a set-valued flow at the singularity. The set-value flow has 2 dimensions in (i) and 3 dimensions in (ii). The cases are: (i) $a_1 = a_2 = -1$ (visible two-fold) with $b_1 < 0$ or $b_2 < 0$ or $b_1 b_2 < 1$; (ii) $a_1 a_2 = -1$ (mixed two-fold) with $b_1 < 0 < b_2$ and $b_1 b_2 < -1$ or with $b_1 + b_2 < 0$ and $b_1 - b_2 < -2$.

a structurally stable system we can perturb this and write

$$\begin{aligned} (\dot{x}_1, \dot{x}_2, \dot{x}_3) &= (F_1, F_2, F_3) + (1-\lambda_1^2)(\alpha, 0, 0) \\ &:= (f_1, f_2, f_3) \,, \end{aligned} \tag{18}$$

for some small constant α, the nonlinear switching term $(1-\lambda_1^2)\alpha$ being permissible because it vanishes for $\lambda_1 = \pm 1$, and hence is consistent with (17).

The switching layer system on $x_1 = 0$, obtained by substituting (17) into (11) for $r = 1$, is

$$(\lambda_1', \dot{x}_2, \dot{x}_3) = (f_1, f_2, f_3) \,. \tag{19}$$

The λ_1' subsystem has equilibria at $\lambda_1 = \mathcal{S}(\lambda_1) = (x_3 - x_2)/(x_3 + x_2) + \mathsf{O}(\alpha)$, which form the sliding manifold

$$\begin{aligned} \mathcal{M}^S = \big\{ &(\lambda_1, x_2, x_3) \in [-1, +1] \times \mathbb{R}^2 \ : \\ &-\tfrac{1+\lambda_1}{2} x_2 + \tfrac{1-\lambda_1}{2} x_3 + \alpha(1-\lambda_1^2) = 0 \big\} \,, \end{aligned} \tag{20}$$

illustrated in figure 5. On $\mathcal{M}^S$ the sliding dynamics is given by

$$(\lambda_1', \dot{x}_2, \dot{x}_3) = \frac{(0, b_2 x_2 + a_1 x_3, a_2 x_2 + b_1 x_3)}{x_3 + x_2} + \mathsf{O}(\alpha) \,. \tag{21}$$

The invariance of $\mathcal{M}^S$ breaks down at the folds (on the boundaries of the switching layer where $\lambda_1 = \pm 1$), and also inside the switching layer where (15) (for $r = 1$) is violated, which simplifies to the condition $\frac{\partial \lambda_1'}{\partial \lambda_1} \neq -\frac{1}{2}(x_2 + x_3) - 2\alpha\lambda_1$. Combining this with (20), the invariance of $\mathcal{M}^S$ breaks down on the set

$$\begin{aligned} \mathcal{L} = \big\{ &(\lambda_1, x_2, x_3) \in \mathcal{M}^S : \\ &\lambda_1 = 2\tfrac{2\alpha + x_3 - x_2}{x_3 + x_2} = -\tfrac{x_3 + x_2}{4\alpha} \in [-1, +1] \big\} \,, \end{aligned} \tag{22}$$

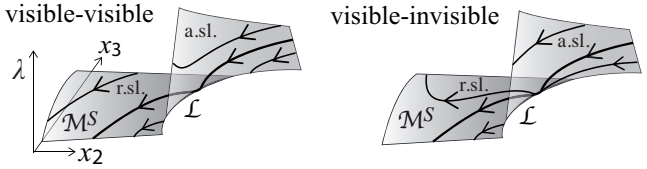

FIG. 5. The sliding manifolds $\mathcal{M}^S$ inside the switching layer for the two cases in figure 4. The curve $\mathcal{L}$ is the set where the vertical (λ) direction lies tangent to $\mathcal{M}$, where the attracting (a.sl.) and repelling (r.sl.) branches meet.

Either side of $\mathcal{L}$, the two-dimensional curved surface $\mathcal{M}^S$ has an attracting branch in an α-neighbourhood of $x_2, x_3 > 0$, where $\frac{\partial \lambda_1'}{\partial \lambda_1}\Big|_{\mathcal{M}^S} < 0$, and a repelling branch in an α-neighbourhood of $x_2, x_3 < 0$, where $\frac{\partial \lambda_1'}{\partial \lambda_1}\Big|_{\mathcal{M}^S} > 0$. The non-hyperbolicity line $\mathcal{L}$ is a curve with tangent vector $e_{\mathcal{L}} = (\,1, 2\alpha(\lambda_1 - 1), -2\alpha(\lambda_1 + 1)\,)$.

This means that the quantity α is vital, because if $\alpha = 0$ then $\mathcal{L}$ aligns precisely with the λ_1' dummy system (i.e. it is vertical in figure 5), constituting a structural instability (of infinite codimension since $\mathcal{L}$ aligns with λ_1 over infinitely many points on $[-1, +1]$), and meaning the sliding dynamics (12) cannot be defined there.

The set $\mathcal{L}$ is the continuation of the two-fold singularity through the switching layer. The perturbation α ensures that this is in a generic position with respect to the flow. A new isolated point singularity may then exist along $\mathcal{L}$, where the flow's projection along the λ_1-direction onto $\mathcal{M}^S$ is indeterminate, defined as the point where

$$f_1 = 0\,, \quad \frac{\partial f_1}{\partial \lambda_1} = 0\,, \quad (f_2, f_3) \cdot \frac{\partial f_1}{\partial (x_2, x_3)} = 0\,. \tag{23}$$

In slow-fast systems (which the switching layer system is due to the dot and prime timescales), such a point is known as a *folded singularity* [30]. By a coordinate transformation that straightens out $\mathcal{L}$ and puts the folded singularity at the origin, as derived in [20], the switching layer system (19) becomes the canonical form of the folded singularity along a slow critical manifold in a two-timescale system [30]

$$\left\{ \begin{array}{rcl} {y_1}' &=& y_2 + y_1^2 + \mathsf{O}\left(y_1 y_3\right)\,, \\ \dot{y}_2 &=& \tilde{b} y_3 + \tilde{c} y_1 + \mathsf{O}\left(y_3^2, y_1 y_3\right)\,, \\ \dot{y}_3 &=& \tilde{a} + \mathsf{O}\left(y_3, y_1\right)\,, \end{array} \right. \tag{24}$$

where

$$\tilde{a} = f_{3s}\,, \quad \tilde{b} = -\left(f_{2s} + f_{3s} - 2\tilde{c}\sqrt{|\alpha|}\right)/4|\alpha|\,,$$
$$\tilde{c} = \left((1 - \lambda_{1s})k_{3s} - (1 + \lambda_{1s})k_{2s}\right)/2\sqrt{|\alpha|}\,,$$

and $f_{2s} = l_{2s} + k_{2s}\lambda_{1s}$, $f_{3s} = l_{3s} + k_{3s}\lambda_{1s}$, $l_{2s} = \frac{1}{2}(a_1 + b_2)$, $l_{3s} = \frac{1}{2}(b_1 + a_2)$, $k_{2s} = \frac{1}{2}(a_1 - b_2)$, $k_{3s} = \frac{1}{2}(b_1 - a_2)$, and λ_{1s} is the solution to (23). As can be seen from the values of these constants, that the transformation to obtain the canonical form is only nonsingular if α in (18) is non-vanishing.

The most important factor in determining the role of such exit points is the dimension of the set-valued orbit through the singularity. As shown in figure 4(i), two visible tangencies give only a single sliding trajectory passes through the two-fold, and the flow generated is two dimensional. This means the set of orbits through the exit point has zero measure in the overall phase space, and is unlikely to play a direct role in local or global dynamics. In figure 6(i) we simulate an example system

$$\begin{array}{l} \mathbf{f}^+ = (-x_2, \frac{2}{5}x_1 + \frac{1}{10}x_2 - 1, \frac{3}{10}x_2 - \frac{1}{5}x_2 x_3 - \frac{2}{5}), \\ \mathbf{f}^- = (x_3, \frac{1}{5}x_2 x_3 - \frac{3}{5}, \frac{2}{5}x_3 - 1 - x_1), \end{array} \tag{25}$$

with $\alpha = 1/5$, which has a two-fold at the origin formed by two visible tangencies. This system contains a re-injection to the neighbourhood of the two-fold, which creates periodic or chaotic dynamics as we vary the coefficients. This verifies that, despite intricate local dynamics, no trajectories pass through the two-fold itself, so the exit point itself does not play a role, though it is the organizing centre of the surrounding attractor.

For one visible and one invisible tangency, on the other hand, a whole family of sliding trajectories pass through the two-fold, generating a three dimensional flow. This is therefore a significant feature in the local flow. As the flow passes through the exit point, its ensuing set-valuedness means that in simulations the system is highly sensitive to perturbations of the model itself, or the method of calculation. As an example take the system

$$\begin{array}{l} \mathbf{f}^+ = (-x_2 + \frac{1}{10}x_1, x_1 - c_1, x_1 - 2), \\ \mathbf{f}^- = (x_3 + c_2 x_1, x_1 + c_3, 1 - x_1), \end{array} \tag{26}$$

again with $\alpha = 1/5$. As in the last example, this contains a re-injection to the neighbourhood of the two-fold. For different coefficients this creates pseudo periodic or chaotic motion that persists over long times, but in this case the orbits pass through the exit point at the two-fold itself, and closed attractors may not exist. Small changes in parameters or the computational method can then result in very different quantitative behaviour due to determinacy-breaking at the two-fold, and figure 6(ii-iii) show two examples (for different parameters given in the caption). In (ii) a chaotic-like motion persists for long times (more than $t = 1500$ in this simulation), while in (iii), after some time $t > 400$ the orbit begins evolving along a canard trajectory that explores the repelling sliding region, and on the second such excursion diverges to infinity.

The numerical solutions in both examples are obtained by approximating $\lambda = \text{sign}\, x_1$ by a sigmoid function $\tanh(x_1/\varepsilon)$ with $\varepsilon = 10^{-7}$, taking an initial point $(x_1, x_2, x_3) = (0.4, 1, 1.4)$ for the simulation. Although the resulting simulations are highly sensitive (including high sensitivity to step sizes, numerical tolerances, and the choice of sigmoid function), different values result in qualitatively similar behaviour.

The implication of (24) existing inside the switching layer is that at the heart of the two-fold singularity lies

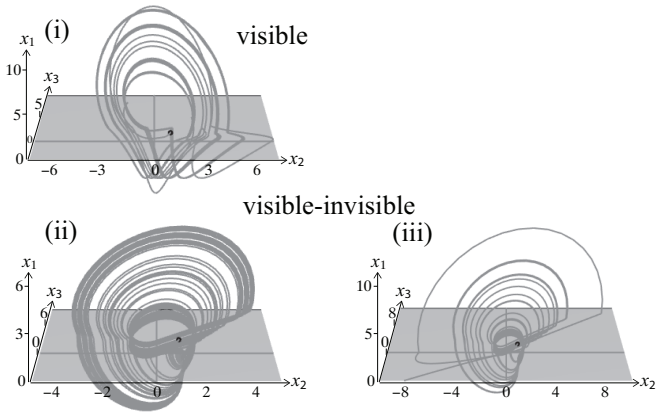

FIG. 6. Three examples of attractor organised around a two-fold singularity; examples based on those in [20]. Showing simulations of: (i) the system (25), (ii-iii) the system (26) with (i) $c_1 = 6/5,\ c_2 = 1/10,\ c_3 = 23/100$, and (ii) $c_1 = 11/10,\ c_2 = 1/20,\ c_3 = 21/100$.

the discontinuous limit of a two timescale folded singularity, of the kind described in [30], responsible for so-called *canard* phenomena. A canard is a trajectory that travels from an attracting to a repelling branch of an invariant manifold, in this case $\mathcal{M}^S$, corresponding to traveling from the attracting to repelling regions of sliding in figure 4. Inside the switching layer with $\alpha \neq 0$ we obtain the critical limit of a generic slow-fast system, corresponding to the critical limit in [8, 30]. The switching layer here reveals this singularity, in its different forms for different parameters, allowing us to interpret determinacy-breaking at the two-fold singularity as the infinite crowding of trajectories that occurs in the singular limit of a deterministic slow-fast system. The different topologies of canards possible may be found in [8, 20, 30].

C. Exit via an intersection: deterministic

Sliding on one switching manifold can also be terminated by transversal intersection with another switching manifold. Even in the simplest example of a codimension $r = 1$ sliding region, terminated by meeting a second switching surface at a codimension $r = 2$ switching intersection (as in figure 3(iii-iv)), there are a huge number of scenarios by which exit can occur in this way. No classification has been attempted to date. Here we describe the typical behaviour that characterises such exit, particularly whether it is deterministic (this section) or determinacy-breaking (in section III D).

Consider, without loss of generality, a sustained interval of sliding on $x_1 = 0 > x_2$, terminated by a second switching surface $x_2 = 0$. A trajectory may exit into one of the two regions $x_1, x_2 > 0$ or $x_2 < 0 < x_1$ (exit into $x_1 < 0$ is impossible because the flow is attracting towards $x_1 = 0 > x_2$ by assumption), or into one of the three switching surface regions $x_1 = 0 < x_2$, $x_2 = 0 < x_1$, $x_2 = 0 > x_1$. Provided that exit is possible into only one of these regions at $x_1 = x_2 = 0$, the system may remain deterministic, in the form represented by figure 3(iii), as we consider below. If exit is possible into more than one such region then determinacy is broken, and we consider that in the next section.

As a structural model of deterministic exit at an intersection, consider the piecewise-constant system

$$(\dot{x}_1, \dot{x}_2) = \begin{cases} \mathbf{f}^{++} = \mathbf{f}^{--} = (1,\ 1) & \text{if } x_1 x_2 > 0, \\ \mathbf{f}^{-+} = \mathbf{f}^{+-} = (1, -1) & \text{if } x_1 x_2 < 0, \end{cases} \tag{27}$$

for which (8) simplifies to

$$(\dot{x}_1, \dot{x}_2) = \tfrac{1}{2}(1 - \lambda_1 + \lambda_2 + \lambda_1\lambda_2,\ 1 + \lambda_1 - \lambda_2 + \lambda_1\lambda_2)\ .$$

Sliding occurs in the regions $x_2 = 0 > x_1$ and $x_1 = 0 > x_2$, and flows towards the switching intersection $x_1 = x_2 = 0$. Crossing occurs on $x_2 = 0 < x_1$ and $x_1 = 0 < x_2$. The result is that all trajectories flow eventually into the region $x_1, x_2 > 0$, and trajectories that slide initially and exit at the intersection do so along a common trajectory $\{x_1(t), x_2(t)\} = \{t, t\}$, $t \geq 0$.

A switching layer system (11) can be taken separately on each region of the switching surface, using $r = 1$ on $x_2 = 0 > x_1$, $x_2 = 0 < x_1$, $x_1 = 0 > x_2$, $x_1 = 0 < x_2$, and using $r = 2$ on the intersection $x_1 = x_2 = 0$. The invariant manifold $\mathcal{M}^S$ exists in the sliding regions on the codimension $r = 1$ switching surfaces. The switching layer system at the intersection is

$$(\lambda_1', \lambda_2') = \tfrac{1}{2}(1 - \lambda_1 + \lambda_2 + \lambda_1\lambda_2,\ 1 + \lambda_1 - \lambda_2 + \lambda_1\lambda_2)\ ,$$

in which the flow converges on the trajectory $\{\lambda_1(\tau), \lambda_2(\tau)\} = \{\tau, \tau\}$, $-1 < \tau < +1$, and the nearby flow carries trajectories from the sliding regions onto the exit trajectory $\{x_1(t), x_2(t)\} = \{t, t\}$, $t \geq 0$.

This is rather simple because it is deterministic, i.e. the flow is single-valued. Various other scenarios may be studied, but they generate little of interest for deeper study here. In particular one may consider

$$\begin{array}{ll} \mathbf{f}^{++} = (-1, 1), & \mathbf{f}^{--} = (1, 1), \\ \mathbf{f}^{-+} = (1, 1), & \mathbf{f}^{+-} = (-1, 1), \end{array}$$

where trajectories slide along $x_1 = 0 > x_2$ into the intersection, and exit via sliding along $x_1 = 0 < x_2$, or

$$\begin{array}{ll} \mathbf{f}^{++} = (2, -1), & \mathbf{f}^{--} = (1, 1), \\ \mathbf{f}^{-+} = (1, -1), & \mathbf{f}^{+-} = (-1, 1), \end{array}$$

where trajectories slide along $x_1 = 0 > x_2$ and $x_2 = 0 > x_1$ into the intersection, and exit via sliding along $x_1 = 0 < x_2$. Both cases are deterministic. An attracting branch of a sliding manifold $\mathcal{M}^S$ exists in each sliding region, and the different branches are connected by trajectories passing through the intersection in finite time. The analysis of these is quite straightforward, and the steps are similar to those above. We describe these steps in more detail for the more interesting case that follows.

D. Exit via a switching intersection: determinacy-breaking

As a structural model of determinacy-breaking exit from codimension $r = 1$ sliding at a codimension $r = 2$ intersection, illustrated in figure 3(iv),

$$(\dot{x}_1, \dot{x}_2, \dot{x}_2) = \begin{cases} \mathbf{f}^{++} = \mathbf{f}^{--} = (1, x_3 + 1, 0) \text{ if } x_1 x_2 > 0, \\ \mathbf{f}^{-+} = \mathbf{f}^{+-} = (1, x_3 - 1, 0) \text{ if } x_1 x_2 < 0, \end{cases} \tag{28}$$

for $|x_3| < 1$. We will show that this exhibits determinacy-breaking, but that the lack of determinacy is partially resolved by the switching layer dynamics. The equality between diagonally opposite vector fields in (28) is for economy here, and has no bearing on the results (small constant, linear, or nonlinear terms can be added to any of the four vector fields without significant effect).

The canopy combination (8) applied to (28) simplifies to

$$(\dot{x}_1, \dot{x}_2, \dot{x}_3) = (1,\ x_3 + \lambda_1 \lambda_2,\ 0) \tag{29}$$

where $\lambda_i = \operatorname{sign} x_i$.

Substituting into (12) with $r = 1$, it is easily seen that trajectories in $x_1 < 0$ reach the intersection in finite time via sliding on $x_2 = 0 \geq x_1$. The trajectories lying on planes $x_2/x_1 = x_3 \pm 1$ reach the intersection directly without sliding. Similarly trajectories in $x_1 > 0$ depart the intersection in finite time via sliding on $x_2 = 0 \leq x_1$, with trajectories on the planes $x_2/x_1 = x_3 \pm 1$ departing directly without sliding.

The line $x_1 = x_2 = 0$ is a determinacy-breaking singularity. From an inspection of the phase portrait outside the surfaces, and the sliding portrait on $x_1 = 0$, it appears (see figure 7(i)) that all trajectories in the region $x_3 - 1 \leq x_2/x_1 \leq x_3 + 1$ pass through the intersection $x_1 = x_2 = 0$, forming a continuum of trajectories all of which flow into and out of the intersection in finite time, and any point in this set with $x_1 < 0$ is connected via the flow to any point in this set with $x_1 > 0$ with the same x_3 value. We shall have to inspect the switching layer dynamics to verify whether all of these orbits actually exist through the intersection, but outside the region $x_3 - 1 \leq x_2/x_1 \leq x_3 + 1$ at least the system is deterministic.

The switching layer system on $x_1 = 0$ for $x_2 \neq 0$, given by (11) with $r = 1$, is

$$(\lambda_1', \dot{x}_2, \dot{x}_3) = (1,\ x_3 + \lambda_1 \operatorname{sign} x_2,\ 0)\ , \tag{30}$$

with $\lambda_1 \in [-1, +1]$. The λ_1' equation is constant, so this system provides a simple transition between the surfaces $\lambda_1 = -1$ and $\lambda_1 = +1$ on the dummy (prime) timescale.

The switching layer system on $x_2 = 0$ for $x_1 \neq 0$, given again by (11) with $r = 1$ but adapted so that the switching surface is $x_2 = 0$, is

$$(\dot{x}_1, \lambda_2', \dot{x}_3) = (1,\ x_3 + \lambda_2 \operatorname{sign} x_1,\ 0)\ , \tag{31}$$

with $\lambda_2 \in [-1, +1]$. The λ_2' equation has a set of x_3-parameterized equilibria $\lambda_2 = -x_3 \text{sign}(x_1)$, which are normally hyperbolic since $\partial \lambda_2'/\partial \lambda_2 = \operatorname{sign} x_1$, forming simple planar invariant surfaces which are attracting for $x_1 < 0$ and repelling for $x_1 > 0$. These are the sliding manifolds

$$\mathcal{M}^S = \left\{ (x_1, \lambda_2, x_3) : \begin{array}{l} x_1 \neq 0,\ |x_3| < 1, \\ \lambda_2 = -x_3 \operatorname{sign}(x_1) \end{array} \right\} \tag{32}$$

of the dynamics on $x_2 = 0$. On $\mathcal{M}^S$ the system obeys the sliding dynamics

$$(\dot{x}_1, 0, \dot{x}_3) = (1,\ x_3 + \lambda_1 \lambda_2,\ 0)\ . \tag{33}$$

This gives a constant drift in the positive x_1 direction on $\mathcal{M}^S$ inside $x_2 = 0$, with $\lambda_2 = -x_3 \text{sign}\, x_1$.

The switching layer system on the intersection $x_1 = x_2 = 0$, given by (12) with $r = 2$, is

$$(\lambda_1', \lambda_2', \dot{x}_3) = (1,\ x_3 + \lambda_2 \text{sign}\, x_1,\ 0)\ , \tag{34}$$

for $\lambda_1, \lambda_2 \in [-1, +1]$, which has solution trajectories satisfying

$$\lambda_2(\lambda_1) = e^{\lambda_1^2/2} \left(\lambda_{20} e^{-\lambda_{10}^2/2} + x_3 \sqrt{\tfrac{\pi}{2}} \times \left\{ \text{Erf}\left[\tfrac{\lambda_1}{\sqrt{2}} \right] - \text{Erf}\left[\tfrac{\lambda_{10}}{\sqrt{2}} \right] \right\} \right)\ . \tag{35}$$

The λ_2' equation in (34) has a nullcline $\lambda_1 \lambda_2 = -x_3$ on which $\frac{\partial \lambda_2'}{\partial \lambda_1} = \lambda_2 = -x_3/\lambda_1$. The nullcline diverges and

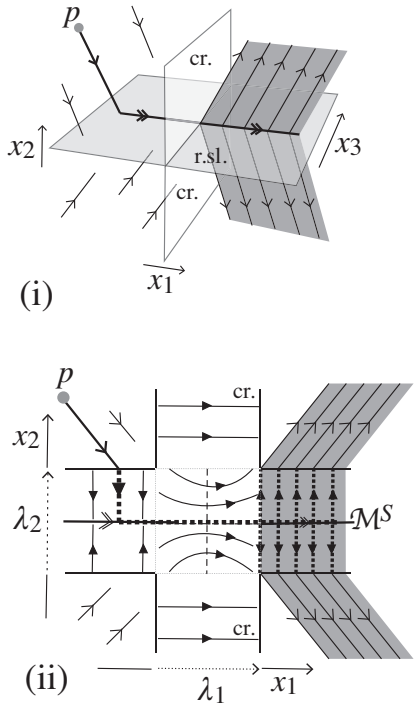

FIG. 7. Determinacy breaking at a switching intersection. (i) shows the discontinuous system, (ii) shows the blow up system in the plane $x_3 = 0$. The trajectory of any point p in $x_1 < 0$ becomes multi-valued as it exits the intersection, identifiable as the set $x_{1,2} = 0$ in (a) and $\lambda_{1,2} \in [-1, +1]$, in (b).

leaves the region $\lambda_{1,2} \in [-1,+1]$, existing only for $|\lambda_{1,2}| > |x_3|$. The nullcline is structurally stable with respect to the flow, having a gradient vector $\left(\frac{\partial}{\partial\lambda_1}, \frac{\partial}{\partial\lambda_2}, \frac{\partial}{\partial x_3}\right)\lambda_2' = (\lambda_2, \lambda_1, 1)$ throughout $\lambda_{1,2} \in [-1,+1]$.

The continuation of the attracting and repelling planes $\lambda_2 = \pm x_3$ in $x_1 \lessgtr \mp 1$ into the region $\lambda_{1,2} \in [-1,+1]$ are given from (35) by

$$\lambda_2(\lambda_1) = x_3 e^{\lambda_1^2/2}\left(\pm e^{-1/2} + \sqrt{\tfrac{\pi}{2}} \times \left\{\mathrm{Erf}\left[\tfrac{\lambda_1}{\sqrt{2}}\right] \pm \mathrm{Erf}\left[\tfrac{1}{\sqrt{2}}\right]\right\}\right), \tag{36}$$

and form the continuation of $\mathcal{M}^S$. This implies that the flow from the attracting plane of $\mathcal{M}^S$ curves towards negative λ_2 in $x < 0$, and towards positive λ_2 in $x_3 > 0$, thus exiting either into the region $x_1, x_2 > 0$ in $x_3 < 0$ or into the region $x_2 < 0 < x_1$ in $x_3 > 0$. In fact, upon reaching either $\lambda_1 = +1$ or $\lambda_2 = +1$, the λ_2' and λ_1' dynamics respectively, given by (31) and (30), drive the flow into the corners $\lambda_1 = +1$, $\lambda_2 = \mathrm{sign}\, x_3$.

The dynamics is illustrated in figure 8 for $x_3 < 0$. The splitting in the x_2 direction between the attracting and repelling manifolds (36) inside the intersection depends linearly on x_3, given by $\delta\lambda_2(\lambda_1) = x_3 e^{\lambda_1^2/2}\left(2e^{-1/2} + \sqrt{2\pi}\,\mathrm{Erf}\left[\frac{1}{\sqrt{2}}\right]\right)$. There exists a unique solution trajectory given by

$$\lambda_1(t) = t\,, \qquad \lambda_2(t) = 0\,, \qquad x_3(t) = 0\,, \tag{37}$$

in the region $\lambda_2 \in [-1,+1]$, valid for all t and hence running along the λ_1 coordinate axis. This is a *canard* trajectory, meaning an orbit that passes from an attracting invariant manifold to a repelling invariant manifold, spending $\mathsf{O}(1)$ time on each. In this case the canard passes from the attracting plane $\lambda_2 = x_3$ for $\lambda_1 < -1$ to the repelling plane $\lambda_2 = x_3$ for $\lambda_1 > +1$. There is only one such trajectory, and it is structurally stable, because the attracting and repelling branches of $\mathcal{M}^S$ intersect transversally at $\lambda_1 = \lambda_2 = x_3 = 0$. Note that the existence of a single canard, rather than every trajectory on $x_2 = 0$ being a canard, is evident only from this switching layer analysis, and cannot be seen by inspecting the dynamics outside the switching surface (figure 7(i)) alone.

One trajectory therefore exists which passes through the intersection and remains asymptotic to $x_2 = 0$ as $x_1 \to \pm\infty$. All trajectories that enter the intersection are expelled via the point $\lambda_1 = +1$, $\lambda_2 = \mathrm{sign}\, x_3$, depending on whether they travel through positive or negative x_3. (Conversely, all trajectories that travel along the repelling sliding region can be followed back in time to the point $\lambda_1 = -1$, $\lambda_2 = -\mathrm{sign}\, x_3$ depending on their x_3 values).

In the (x_1, x_2) plane, if we take x_3 as a parameter, the structural model above shows that different values of x_3 give qualitatively different dynamics, and determinacy-breaking occurs only at $x_3 = 0$. In three dimensions the different scenarios unfold to create a structurally stable singularity, and at its heart, a canard trajectory

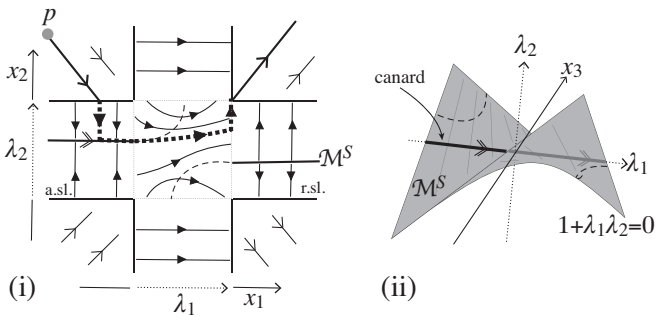

FIG. 8. Sketch of the switching layer system for simple exit from a crossing of switching surfaces. In (ii) we show the layer of the intersection, as well as the switching layers along $x_1 = 0$ (for $x_2 \neq 0$) and $x_2 = 0$ (for $x_1 \neq 0$), and the dynamics outside the switching surfaces, the case shown is in a coordinate plane with constant $x_3 < 0$; and in (i) we show the invariant manifold $\mathcal{M}^S$ inside the switching layer of the intersection point $x_1 = x_2 = 0$.

(37) through the intersection, hidden inside the switching layer.

Numerous other scenarios exhibit similar behaviour and yield to similar analysis, consider for example $\mathbf{f}^{--} = (1, x_3 + 1, 0)$, $\mathbf{f}^{+-} = (1, -1, 0)$, and $\mathbf{f}^{-+} = (-1, -2, 0)$, with either $\mathbf{f}^{++} = (1, 3, 0)$ or $\mathbf{f}^{++} = (-1, 2, 0)$, in both of which there is similar determinacy-breaking passage through the intersection, which can be resolved except at a special value of x_3; in these examples there is also re-injection of the set-valued flow back into the singularity, resulting in complex oscillatory dynamics in the neighbourhood of the intersection.

We shall not look in detail at these examples, but we conclude with a simulation to demonstrate the effect of such a determinacy-breaking exit point. Consider the system

$$\begin{pmatrix}\dot{x}_1\\ \dot{x}_2\\ \dot{x}_3\end{pmatrix} = \begin{pmatrix}1 - \lambda_2 x_2 + \frac{1}{5}\lambda_1\\ x_3 + \lambda_1\lambda_2 - c\lambda_2\\ -\frac{1}{10}x_3 - \frac{1}{5}x_2\end{pmatrix} \tag{38}$$

where c is a constant in the range $0 < c < 1$. This provides an example of the global dynamics induced by a local singularity of the form (28), having the same qualitative phase portrait near the intersection $x_1 = x_2 = 0$.

First, observe that there is little qualitative difference between the phase portraits (figure 9) of (38) for different c. The simulations below will reveal that very different dynamics, however, is seen depending on c, due to sensitivity in the flow's exit from the intersection.

In figure 10 we simulate (38) by approximating $\lambda_i = \mathrm{sign}\, x_i$ with $\phi(x_i/\varepsilon) = \tanh(x_i/\varepsilon)$ for $i = 1, 2$, with $\varepsilon = 10^{-4}$. The result is periodic or chaotic dynamics that enters the origin by sliding along $x_1 < 0 = x_2$, then exits into positive x_2 for $x_3 > 0$ and into negative x_2 for $x_3 < 0$ (this is verified from closer inspection of the simulations, not shown). This is as predicted from the switching layer analysis above. The result in (i) is a simple periodic orbit, and as we vary c the period of this attractor changes

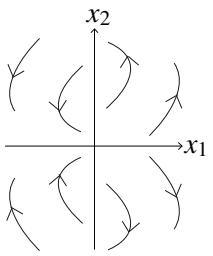

FIG. 9. The flow of (29) with two switches. The phase portrait does not change qualitatively outside the switching surfaces $x_1x_2 = 0$ for different values of c.

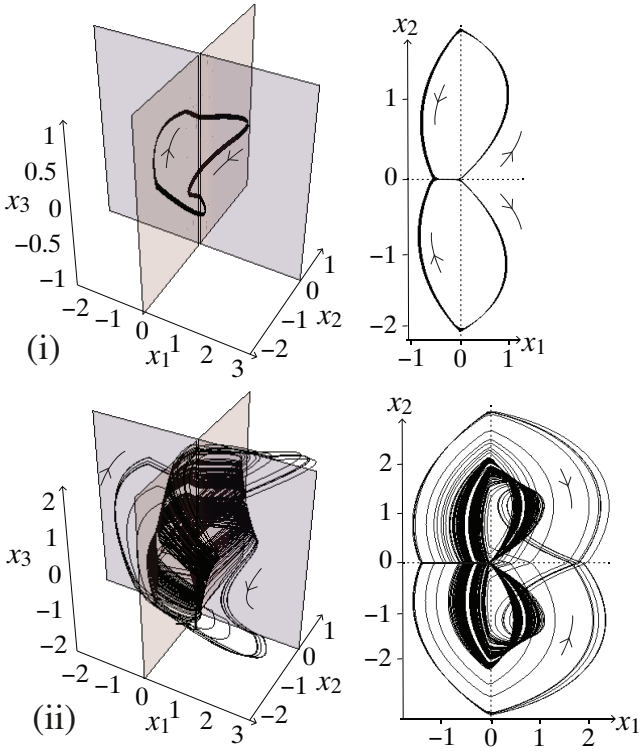

FIG. 10. An attractor driven through an intersection exit point: a simulation of (38) with (i) $c = \frac{3}{10}$ and (ii) $c = \frac{2}{5}$. The full three dimensional simulation and its projection into the (x_1, x_2) plane are shown.

rapidly, becoming eventually the complex attractor in (ii). (In (ii-b) trajectories are also seen that cross the half-plane $x_2 = 0 < x_1$, which have strayed to large enough x_3 that $x_2 = 0$ is no longer a sliding region, so the flow crosses through transversally). Any trajectories that pass through $x_1 = 0$ cross it transversally (in the positive x_1 direction near the intersection, but also in the negative x_1 direction at large x_3 values which allows the flow in (ii) to loop around more intricately), and any trajectories that hit the half-plane $x_2 = 0 > x_1$ do so at small enough x_3 that they then slide along $x_2 = 0$ into the singularity.

To verify that the dynamics observed is a result of the singularity geometry, and not of the choice of smoothing in the simulation, we can simulate the same system for the same parameters, but approximate the switch by different sigmoid functions (we could also take different values of $0 < \varepsilon \ll 1$, and introduce hysteresis, delay, or noise, with similar results).

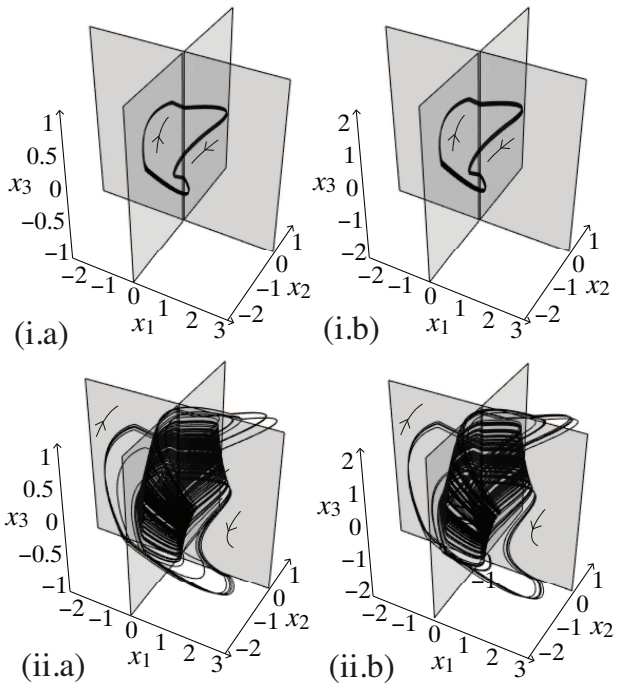

FIG. 11. The attractors in figure 10 for the smooth rational (a) and ramp (b) smoothings described in the text, with parameters and initial conditions corresponding to those in figure 10.

In figure 11 we repeat the simulation (showing only the three dimensional image) with the polynomial function $\phi(x_i/\varepsilon) = (x_i/\varepsilon)/\sqrt{1 + (x_i/\varepsilon)^2}$, and the continuous but non-differentiable ramp function $\phi(x_i/\varepsilon) = \text{sign}(x_i)$ for $|x_i| > \varepsilon$ and $\phi(x_i/\varepsilon) = x_i/\varepsilon$ for $|x_i| \leq \varepsilon$. These demonstrate that the choice of smoothing has no significant effect upon the dynamics, and is not responsible for the complex dynamics observed.

We have considered what happens when a codimension $r = 1$ sliding flow arrives either at a tangency or a codimension $r = 2$ intersection. A codimension $r = 1$ sliding trajectory will not generically encounter an intersection of codimension $r \geq 3$ (i.e. where three or more switching manifolds intersect), therefore this completes our study of the basic generic mechanisms for exit from codimension $r = 1$ sliding.

IV. EXIT FROM CODIMENSION TWO SLIDING

As we add more dimensions, and more switches, phenomena will occur at higher codimension that are analogous to the four kinds analysed above. For example, trajectories sliding along an intersection with codimension $r = 2$ may exit to codimension $r = 1$ sliding, by

intersection a third switching manifold, analogous to the cases in sections III C-III D. In the section below we look at the less obvious scenario of how tangential exit points extend to higher codimensions, for which the principles above extend rather powerfully, but we also consider a new case that is introduced, that of exit by spiralling around a codimension $r = 2$ sliding region.

A. Tangential exit from an intersection

To study exit from sliding via a simple tangency of the flow to an intersection, take as a structural model

$$(\dot{x}_1, \dot{x}_2, \dot{x}_3) = \begin{cases} \mathbf{f}^{++} = (x_3 + 1, -1, 1) & \text{if} \quad 0 < x_1, x_2, \\ \mathbf{f}^{-+} = (1\ ,\ -1\ ,\ 0\ ) & \text{if} \quad x_1 < 0 < x_2, \\ \mathbf{f}^{+-} = (-1\ ,\ 1,\ 0\ ) & \text{if} \quad x_2 < 0 < x_1, \\ \mathbf{f}^{--} = (1\ ,\ 1\ ,\ 0\ ) & \text{if} \quad x_1, x_2 < 0, \end{cases} \tag{39}$$

whose geometry is sketched in figure 12, for $x_3 > -1$.

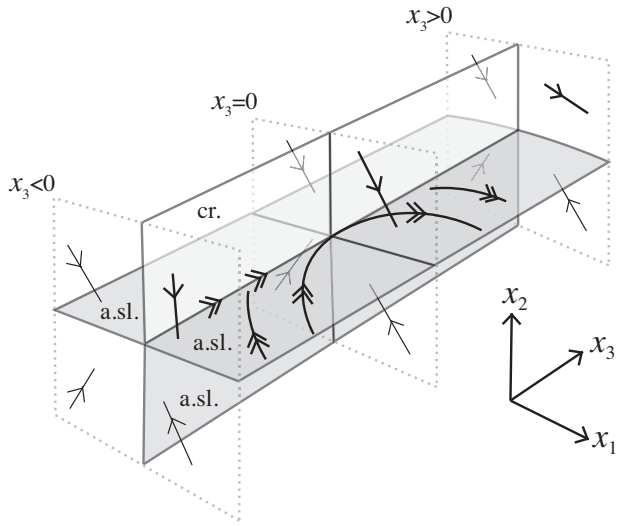

FIG. 12. Sketch of the system with vector fields (39), showing projections of the vector fields into three constant x_3 planes, and the sliding dynamics on three half-planes and on the intersection.

The canopy (6) of the component vector fields $\mathbf{f}^{\pm\pm}$ gives

$$(\dot{x}_1, \dot{x}_2, \dot{x}_3) = \tfrac{1+\lambda_2}{2}\left(\tfrac{1+\lambda_1}{2}x_3 + 1, -1, \tfrac{1+\lambda_1}{2}\right) + \tfrac{1-\lambda_2}{2}(-\lambda_1, 1, 0) \tag{40}$$

with $\lambda_1, \lambda_2 \in [-1, +1]$, and $\lambda_i = \operatorname{sign} x_i$ for $x_1, x_2 \neq 0$.

First let us find the dynamics of the codimension $r = 1$ surfaces, i.e. excluding the intersection. By applying (12)-(13) for $r = 1$ on $x_1 = 0$ and $x_2 = 0$ separately, to derive sliding modes if they exist, we find:

- $x_1 = 0 < x_2$ is a crossing region for $x_3 < 1$ since $f_1^{++} f_1^{-+} = 1 + \mathsf{O}(x_3) > 0$;
- $x_1 = 0 > x_2$ is a sliding region since $f_1^{+-} f_1^{--} = -1 < 0$, the sliding modes satisfy $\lambda_1 = \mathcal{S}(\lambda_1) = 0$, giving a sliding system $(\lambda_1', \dot{x}_2, \dot{x}_3) = (0, 1, 0)$;
- $x_2 = 0 \neq x_1$ is a sliding region since $f_2^{++} f_2^{+-} = -1 < 0$ on $x_2 = 0 < x_1$ and $f_2^{-+} f_2^{--} = -1 < 0$ on $x_2 = 0 > x_1$, the sliding modes in both regions satisfy $\lambda_2 = \mathcal{S}(\lambda_2) = 0$, giving sliding systems $(\dot{x}_1, \lambda_2', \dot{x}_3) = (x_3, 0, 1)$ and $(\dot{x}_1, \lambda_2', \dot{x}_3) = (1, 0, 0)$ respectively.

At the intersection $x_1 = x_2 = 0$, applying (12)-(13) with $r = 2$, sliding modes exist only for $x_3 < 0$, with $(\lambda_1, \lambda_2) = \mathcal{S}(\lambda_1, \lambda_2) = ((x_3 + 2)/(x_3 - 2), 0)$, giving one dimensional dynamics $(\lambda_1', \lambda_2', \dot{x}_3) = (0, 0, 1)/(2 - x_3)$.

The outcome of the sliding analysis is that trajectories in $x_3 < 0$ are attracted onto the sliding surfaces $x_1 = 0 > x_2$ and $x_2 = 0 \neq x_1$, and thence attracted onto the intersection $x_1 = x_2 = 0$ where they travel towards the origin. At the origin the intersection ceases to admit sliding, and trajectories exit along the sliding system $(\dot{x}_1, \lambda_2', \dot{x}_3) = (x_3, 0, 1)$ on $x_2 = 0 < x_1$, which at the origin is tangent to the intersection as sketched in figure 12.

As for the visible tangency in section III A, here we have a visible tangency of the sliding flow to the intersection, and the exit is deterministic. Let us briefly analyse what happens inside the switching layer in analogy to section III A.

The switching layer system (11) on $x_1 = 0$ is

$$(\lambda_1', \dot{x}_2, \dot{x}_3) = \begin{cases} \left(\tfrac{1}{2}(1 + \lambda_1)\, x_3 + 1, \right. \\ \qquad \left. -1, \tfrac{1}{2}(1 + \lambda_1)\right) & \text{if} \quad x_2 > 0\ , \\ (-\lambda_1, 1, 0) & \text{if} \quad x_2 < 0\ , \end{cases} \tag{41}$$

with $\lambda_1 \in [-1, +1]$, illustrated in figure 13. For $x_2 < 0$ the set $\lambda_1 = 0$ forms an attracting sliding manifold $\mathcal{M}^S$, whose sliding vector field $(\lambda_1', \dot{x}_2, \dot{x}_3) = (0, 1, 0)$, so all trajectories flow into the intersection in finite time. For $x_2 > 0$ there is no sliding, instead the dummy system $\lambda_1' = 1 + \mathsf{O}(x_3)$ carries the flow across the switching surface in the direction of increasing x_2, at least for small x_3.

The switching layer system on $x_2 = 0$ is

$$(\dot{x}_1, \lambda_2', \dot{x}_3) = \begin{cases} \left(\tfrac{1}{2}(1 + \lambda_2)\, x_3 + \lambda_2, \right. \\ \qquad \left. -\lambda_2, \tfrac{1}{2}(1 + \lambda_2)\right) & \text{if} \quad x_1 > 0\ , \\ (1, -\lambda_2, 0) & \text{if} \quad x_1 < 0\ , \end{cases} \tag{42}$$

with $\lambda_2 \in [-1, +1]$. The set $\lambda_2 = 0$ forms an attractive sliding manifold $\mathcal{M}^S$ for all $x_1 \neq 0$ and all x_3, on which the sliding vector field is $(\dot{x}_1, \lambda_2', \dot{x}_3) = (x_3/2, 0, 1/2)$ for $x_1 > 0$ and $(1, 0, 0)$ for $x_1 < 0$. The $\dot{x}_1$ component implies that the sliding flow enters the intersection from $\mathcal{M}^S$ for $x_3 < 0$, but for $x_3 > 0$ crosses through the intersection in the direction of increasing $\dot{x}_1$ along $\mathcal{M}^S$.

The attraction of dynamics towards $x_1 = 0$ and $x_2 = 0$ implies that the switching layer there should possess a sliding manifold $\mathcal{M}^S$ for $x_3 < 0$. The switching layer system on the intersection $x_1 = x_2 = 0$, given by (11) with $r = 2$, is

$$(\lambda_1', \lambda_2', \dot{x}_3) = \tfrac{1+\lambda_2}{2}\left(\tfrac{1+\lambda_1}{2}x_3 + 1, -1, \tfrac{1+\lambda_1}{2}\right) + \tfrac{1-\lambda_2}{2}(-\lambda_1, 1, 0) \tag{43}$$

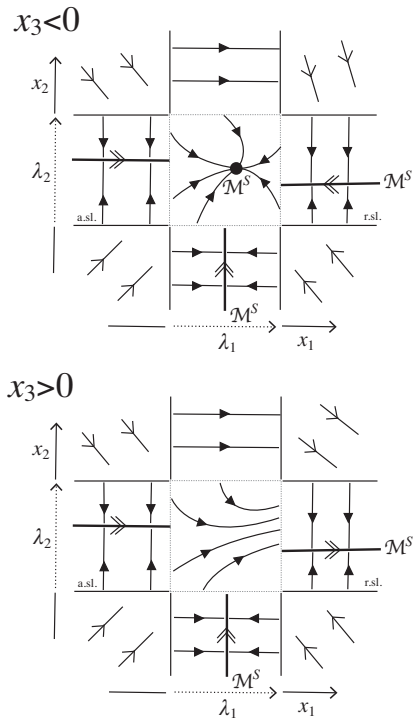

FIG. 13. Sketch of the switching layer dynamics of the system (39), showing an attracting sliding manifold $\mathcal{M}^S$ consisting of curves in the regions $x_2 = 0 < x_1$, $x_2 = 0 > x_1$ and $x_1 = 0 > x_2$, and a point inside $x_1 = x_2 = 0$ for $x_3 < 0$ (this refers to curves and points in $\mathbb{R}^2$, which are of course surfaces and curves respectively in the full $\mathbb{R}^3$).

with $\lambda_1, \lambda_2 \in [-1, +1]$. For $x_3 < 0$ this has an attracting sliding manifold $\mathcal{M}^S$ consistent with (14) along the line $\lambda_1 = \frac{2+x_3}{2-x_3}$, $\lambda_2 = 0$, along which the flow follows the one dimensional system $\dot{x}_3 = 1/(2 - x_3)$. When the flow enters the intersection in the region $x_3 < 0$ it collapses onto $\mathcal{M}^S$ and travels towards $x_3 = 0$, where $\mathcal{M}^S$ leaves the region $\lambda_1, \lambda_2 \in [-1, +1]$. Inside the intersection the flow is still attracted towards the line $\lambda_2 = 0$ on which $\lambda_1' = \frac{1}{2}(1 - \lambda_1) + \frac{1}{4}x_3(1 + \lambda_1)$ is strictly positive for $x_3 > 0$, directing the flow out of the intersection into sliding on the switching surface $\mathcal{M}^S$ on the switching surface $x_1 > 0$, $x_2 = 0$.

As in the previous cases, one may construct many other examples that exhibit similar behaviour, the only key features being that a sliding mode exists on the intersection for some values of x_3, at the boundary of which one of the sliding flows has a visible tangency to the intersection, and the exit of the sliding mode corresponds to an equilibrium exiting from the switching layer of the intersection. The exit is deterministic.

One may build up a hierarchy of intersections and sliding modes of successively higher codimension r, and exit points from the intersections via tangency of the codimension $r - 1$ sliding vector field. By a series of such points a trajectory my cascade down from sliding along a high codimension intersection to lower and lower codimension, eventually releasing from the switching surface altogether. Each of these exit events should behave similar to that above, that is, deterministically, and each decreasing the sliding codimension by one. Coincidences of many such events could decrease the codimension by more than one, however, accompanied by determinacy-breaking, as in the following section.

B. Two-fold exit from an intersection

To study a double tangency to an intersection, consider the structural model

$$(\dot{x}_1, \dot{x}_2, \dot{x}_3, \dot{x}_4) = \begin{cases} \mathbf{f}^{++} = (1 + x_3,\ -1,\ a_1,\ b_1) \\ \qquad\qquad \text{if} \quad 0 < x_1, x_2, \\ \mathbf{f}^{-+} = (+1,\ -1,\ 0,\ 0\ ) \\ \qquad\qquad \text{if} \quad x_1 < 0 < x_2, \\ \mathbf{f}^{+-} = (-1,\ +1,\ 0,\ 0\ ) \\ \qquad\qquad \text{if} \quad x_2 < 0 < x_1, \\ \mathbf{f}^{--} = (d - x_4, -d,\ b_2,\ a_2\ ) \\ \qquad\qquad \text{if} \quad x_1, x_2 < 0, \end{cases} \tag{44}$$

in terms of constants $a_i = \pm 1$ and $b_i \in \mathbb{R}$. It is necessary here to consider four dimensions, as multiple tangencies to a switching intersection do not occur generically in $\mathbb{R}^3$. The constants d, v_1, v_2, can each take values ± 1. We restrict attention to a neighbourhood of the origin $|x_3| < 1,\ |x_4| < 1$.

Figure 14 illustrates the basic dynamics in the x_1, x_2, plane in different regions of x_3, x_4, space. Of the four regions of the switching surface $\{x_1 = 0 < x_2\}$, $\{x_1 = 0 > x_2\}$, $\{x_2 = 0 < x_1\}$, $\{x_2 = 0 > x_1\}$, two exhibit crossing, and two exhibit sliding. For $d = -1$ the two sliding regions are coplanar (on $x_1 = 0$), for $d = +1$ they are orthogonal.

- The coplanar case $d = -1$:

  At $x_1 = 0$ the flow crosses the switching surface if we restrict to $x_3, x_4 > -1$, since then $f_1^{++} f_1^{-+} = 1 + x_3 > 0$ in $x_2 > 0$ and $f_1^{+-} f_1^{--} = 1 + x_4 > 0$ in $x_2 < 0$.

  The $x_2 = 0$ hyperplane is an attracting sliding region for all $x_2 \neq 0$ since $f_2^{++} f_2^{+-} = -1 < 0$ in $x_1 > 0$ and $f_2^{-+} f_2^{--} = -1 < 0$ in $x_1 < 0$. The sliding modes from (13) are given by $\mathcal{S}(\lambda_2) = 0$, and give dynamics

$$(\dot{x}_1, \dot{x}_2, \dot{x}_3, \dot{x}_4) = \begin{cases} (x_3, 0, a_1, b_1)/2 \\ \qquad \text{if} \quad \mathrm{x}_1 > 0\ , \\ (-x_4, 0, b_2, a_2)/2 \\ \qquad \text{if} \quad \mathrm{x}_1 < 0\ , \end{cases} \tag{45}$$

  on $x_2 = 0$.

  The intersection exhibits sliding for $x_3 x_4 > 0$. By (13) the sliding modes are given by $\mathcal{S}(\lambda_1) = \frac{x_4 - x_3}{x_4 + x_3}$ and $\mathcal{S}(\lambda_2) = 0$ (recall by (13) these must both be

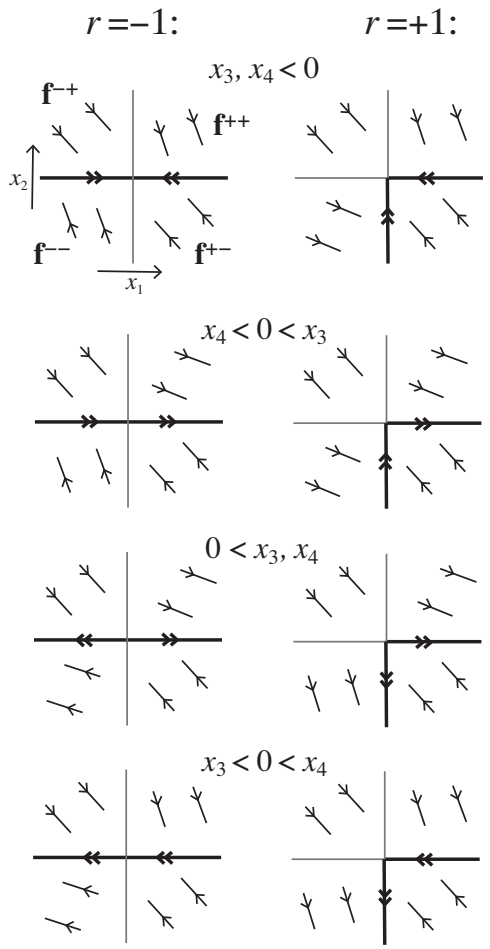

FIG. 14. Sketch of x_1-x_2 dynamics and sliding. As x_3 and x_4 change sign the fields $\mathbf{f}^{00}$ and $\mathbf{f}^{--}$ rotate, and their directions relative to $\mathbf{f}^{+-}$ and $\mathbf{f}^{-+}$ change whether the sliding vector fields point towards or away from the intersection $x_1 = x_2 = 0$.

inside $[-1,+1]$ hence they exist only for $x_3x_4 > 0$), giving dynamics

$$(\dot{x}_4, \dot{x}_4) = \frac{(a_1x_4 + b_2x_3, a_2x_3 + b_1x_4)}{j(x_3, x_4)} \tag{46}$$

on $x_1 = x_2 = 0$, where $j(x_3, x_4) = 2(x_3 + x_4)$ satisfies $x_3, x_4 > 0 \Rightarrow j(x_3, x_4) > 0$ and $x_3, x_4 < 0 \Rightarrow j(x_3, x_4) < 0$. For $x_3x_4 < 0$ the flow therefore crosses through the intersection, from one sliding region to another. There exists a singularity at $x_3 = x_4 = 0$ where these sliding modes are undefined.

- The orthogonal case $d = +1$:

  On $x_1 = 0$, for $x_2 > 0$ the flow crosses the switching surface since $f_1^{++}f_1^{-+} = 1 + x_3 > 0$. For $x_2 < 0$ we have $f_1^{+-}f_1^{--} = x_4 - 1 < 0$, which by (13) has sliding modes $\mathcal{S}(\lambda_1) = \frac{x_4}{x_4-2}$, with dynamics

$$(\dot{x}_2, \dot{x}_3, \dot{x}_4) = \frac{(-x_4, b_2, a_2)}{2 - x_4} \tag{47}$$

on $x_1 = 0 > x_2$.

On $x_2 = 0$, for $x_1 < 0$ the flow crosses the switching surface since $f_2^{-+}f_2^{--} = 1 > 0$. For $x_1 > 0$ we have $f_2^{++}f_2^{+-} = -1 < 0$, which by (13) has sliding modes $\mathcal{S}(\lambda_2) = 0$, giving dynamics

$$(\dot{x}_1, \dot{x}_3, \dot{x}_4) = (x_3, 0, a_1, b_1)/2$$

on $x_2 = 0 < x_1$.

Both of these sliding regions are attracting. The intersection exhibits sliding for $x_3x_4 > 0$, where the sliding modes satisfy $\mathcal{S}(\lambda_1) = 2x_4/j(x_3, x_4)$ and $\mathcal{S}(\lambda_2) = -2x_3/j(x_3, x_4)$, giving

$$(\dot{x}_3, \dot{x}_4) = \frac{(a_1x_4 + b_2x_3, a_2x_3 + b_1x_4)}{j(x_3, x_4)}$$

on $x_1 = x_2 = 0 < x_3x_4$, where $j(x_3, x_4) = \frac{-4x_3x_4}{x_3+x_4+\sqrt{(x_3+x_4)^2+4x_3x_4}}$ and $x_3x_4 > 0 \Rightarrow j(x_3, x_4) > 0$. For $x_3x_4 < 0$ the flow crosses through the intersection from one sliding region to another.

The flow curvature towards or away from the intersection is characterised by $\ddot{x}_1 = a_1$ for $x_2 = 0 < x_1$ along the set $x_3 = 0$ in both cases, and by $\ddot{x}_1 = -a_2$ or $\ddot{x}_2 = -a_2$ on $x_2 = 0 > x_1$ or $x_1 = 0 > x_2$ as appropriate, along the set $x_4 = 0$. The result is that both tangencies are of *visible* type for $a_1 = a_2 = +1$ (curving away from the intersection in both sliding regions), *invisible* type for $a_1 = a_2 = -1$ (curving towards the intersection in both sliding regions), and of mixed type for $a_1a_2 = -1$ (one curves towards and one away from the intersection in either sliding region). This curvature also implies, as seen in figure 14, that the intersection is attracting with respect to the sliding dynamics for $x_3, x_4 < 0$, repelling for $x_3, x_4 < 0$, while the flow crosses between sliding regions at the intersection for $x_3x_4 < 0$.

The switching between the two sliding regions, each of dimension three on (x_1, x_3, x_4) or (x_2, x_3, x_4) space, closely mimics the switching between two regions on (x_1, x_2, x_3) space in the two-fold of section III B; an example comparable to figure 4 is sketched in figure 15. In fact, the sliding vector field on the intersection given by (45) and (47) on (x_3, x_4) space, both expressible as

$$(\lambda_1', \lambda_2', \dot{x}_3, \dot{x}_4) \propto \frac{(0, 0, b_2x_3 + a_1x_4,\ a_2x_3 + b_1x_4)}{j(x_3, x_4)}\,, \tag{48}$$

are equivalent up to time scaling to the canonical form sliding vector field of a two-fold singularity on the switching surface $x_1 = 0$ of a system in (x_1, x_2, x_3) space, namely (21). Note we neglect the term of order α from (21) here; we will remark on this below.

The system of sliding resulting from (44) differs from the two-fold in one important aspect, the sign of the time scaling $j(x_3, x_4)$. That time scaling crucially changes the character of the singularity at $x_3 = x_4 = 0$. The singularity for the 'coplanar' case $d = +1$ may be called

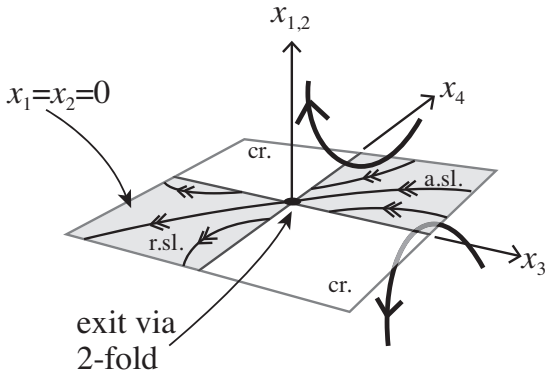

FIG. 15. Sketch of x_3-x_4 sliding dynamics. The visible-visible case of folds is shown with a saddle-like case of sliding dynamics. A complete catalogue of the possible two-dimensional sliding topologies in this codimension $r = 2$ surface is equivalent to the two-dimensional sliding phase portraits for the codimension $r = 1$ two-folds in [7].

a *bridge point*, forming a bridge between attracting and repelling sliding regions, while for the 'orthogonal' case $d = -1$ it may be called a *jamming* point, an equilibrium that the flow may reach or depart in *finite* time. This is shown as follows.

The phase portraits of (48) are that of a linear equilibrium at $x_3 = x_4 = 0$, which takes the form of a node, focus, or saddle depending on a_i and b_i. Because of the time scaling this is actually a false equilibrium, and we must consider how $j(x_3, x_4)$ affects the dynamics nearby. For $d = +1$, similar to the two-fold singularity, the time scaling is positive in the attracting sliding region and negative in the repelling sliding region, becoming zero at the origin such that the vector field remains finite and nonzero there, permitting the flow to pass in finite time from one sliding region to another. For $d = -1$ the time scaling is strictly negative in both sliding regions, becoming zero at the origin such that the vector field remains finite and nonzero, so if they are attracted to repelled from the singularity, they reach/depart it in finite time.

This comparison to the two-fold singularity reveals something else about the character of the singularity at the origin of the system above, namely that the system is structurally unstable at the singularity, and exhibits determinacy-breaking. It also suggests that structural stability requires the addition of a nonlinear term $(1 - \lambda^2)(\alpha, 0, 0, 0)$ for some small α. For brevity we refer the reader to [20] for the straightforward steps to obtain the switching layer on the intersection for the system above, obtaining the invariant sliding manifolds $\mathcal{M}^S$ that connect at $x_3 = x_4 = 0$ and do so in a structurally stable way only for $\alpha \neq 0$, and ultimately, obtaining equivalence by coordinate transformation of the sliding dynamics to the folded singularities of slow-fast systems.

More intriguingly, these open the way to considering p-fold singularities for $p \geq 2$. In an n dimensional system, at the intersection of r switching surfaces, there will generically occur sets of dimension $d = n - k$ where $k \leq 2r$ codimension $r - 1$ sliding flows are tangent to the intersection. We present an example in section V, and the complex dynamics that results.

C. Zeno exit from an intersection

Exit without tangency is also possible. Filippov discussed a planar piecewise constant example in [13], stating that it exhibited geometric convergence, or the Zeno phenomenon, meaning that infinite switches occur as the switching intersection is reached in finite time (the system is so simple yet compelling that it has no doubt been considered elsewhere in literature this author is unaware of). Filippov also noted that this constituted a form of determinacy-breaking when the intersection is repelling. In [11] the scenario was studied for perhaps the first time in three dimensions, highlighting the computational problem raised by spiralling exit from an intersection. We bring together these observations here, showing that the Zeno phenomenon continues to apply as the Zeno set (the intersection) changes stability in a three dimensional system, creating first a codimension two sliding attractor, followed by a determinacy-breaking exit.

Again in three dimensions and with two switching surfaces, we consider the structural model

$$(\dot{x}_1, \dot{x}_2, \dot{x}_3) = \begin{cases} \mathbf{f}^{++} = (x_3 + 1, -1, 1) & \text{if } \ 0 < x_1, x_2 \ , \\ \mathbf{f}^{-+} = (+1 \quad , +1, 0) & \text{if } \ x_1 < 0 < x_2 \ , \\ \mathbf{f}^{+-} = (-1 \quad , -1, 0) & \text{if } \ x_2 < 0 < x_1 \ , \\ \mathbf{f}^{--} = (-1 \quad , +1, 0) & \text{if } \ x_1, x_2 < 0 \end{cases} \tag{49}$$

restricted to $x_3 > -1$. The simplicity of this has no qualitative bearing on the results, but greatly simplifies the calculations.

There is no sliding on the surfaces $x_1 = 0$ or $x_2 = 0$ outside their intersection, as is easily shown from the switching layer systems on the different surfaces $x_1 = 0 \neq x_2$ and $x_2 = 0 \neq x_1$, or performing standard Filippov analysis, either of which show that no sliding modes exist. Instead, the flow spirals around the intersection $x_1 = x_2 = 0$ by crossing through the switching planes, spiralling in towards the intersection for $x_3 < 0$ and away from it for $x_3 > 0$. Only the intersection point itself is then of interest.

The canopy combination (6) applied to (49) simplifies to

$$\mathbf{f} = \left(\lambda_2 + \tfrac{1}{4}x_3(1 + \lambda_1)(1 + \lambda_2), -\lambda_1, \tfrac{1}{4}(1 + \lambda_1)(1 + \lambda_2)\right) \ , \tag{50}$$

and the switching layer system at the intersection, given by (11) with $r = 2$, is

$$\begin{aligned} \lambda_1' &= \lambda_2 + \tfrac{1}{4}x_3(1 + \lambda_1)(1 + \lambda_2) \ , \\ \lambda_2' &= -\lambda_1 \ , \\ \dot{x}_3 &= \tfrac{1}{4}(1 + \lambda_1)(1 + \lambda_2) \ . \end{aligned} \tag{51}$$

The dummy timescale (prime) system has equilibria at $(\lambda_1, \lambda_2) = (0, -\frac{x_3}{x_3+4})$, forming a sliding manifold $\mathcal{M}^S$

on which the sliding dynamics is given by $\dot{x}_3 = 1/(4 + x_3)$. The Jacobian derivative of the equilibrium in the (λ_1, λ_2) variables is $\begin{pmatrix} \frac{x_3}{x_3+4} & 1+\frac{1}{4}x_3 \\ -1 & 0 \end{pmatrix}$, which for $x_3 > -1$ has complex eigenvalues. For $x_3 < 0$ the eigenvalues have negative real part, implying an attracting focus. For $x_3 > 0$ the eigenvalues have positive real part, implying a repelling focus. A drift along in the positive x_3 direction remains. So if a trajectory enters the intersection in $-1 < x_3 < 0$ it will spiral around in the (λ_1, λ_2) coordinates of the switching layer system, initially with decreases radius around $(\lambda_1, \lambda_2) = (0, -\frac{x_3}{x_3+4})$ until it passes into $x_3 > 0$, then begins spiralling outward until it reaches $|\lambda_1| = 1$ or $|\lambda_2| = 1$ and then exits.

Thus when a trajectory enters the intersection $x_1 = x_2 = 0$ for $x_3 < 0$, it does so with a unique value of (λ_1, λ_2) lying on the set

$$\mathcal{B} = \left\{(\lambda_1, \lambda_2) \in [-1, +1]^2 : \ (\lambda_1^2 - 1)(\lambda_2^2 - 1) = 0\right\} \ .$$

We can integrate (51) to find that λ_1 and λ_2 evolve through the region $(\lambda_1, \lambda_2) \in [-1, +1]$ until they again reach the bounding box $\mathcal{B}$, at which exit from the intersection occurs in $x_3 > 0$.

The dynamics *inside* the intersection is therefore well defined, but the entry and exit trajectories in $x_1 x_2 \neq 0$ may not be. In this case, indeed, it is the dynamics outside the intersection that turns out to be the most interesting. The exit from (and entry into) the intersection exhibit a Zeno phenomenon, which we can show as follows.

Take a starting point $(x_1, x_2, x_3) = (0, \xi, \zeta)$ with $\xi > 0$ and $-1 < \zeta < 0$ at time $t = 0$ on one of the switching planes, and say its orbit crosses successive switching planes at times $t = t_1, t_2, t_3, t_4$. The map over time $t = 0$ to $t = t_4$ gives a return map on the half plane $x_1 = 0 < x_2$. In $0 < x_1, x_2$ we have $\dot{x}_2 = -1$ so to reach $x_2 = 0$ takes at time $t_1 = \xi$, arriving at $x_1(t_1) = \int_0^{\xi}(x_3+1)dt = \int_{\zeta}^{\xi+\zeta}(x_3+1)dx_3 = (\frac{1}{2}\xi+\zeta+1)\xi$ and $x_3(t_1) = \xi + \zeta$. The next two sectors are a reflection so we arrive at $(-(\frac{1}{2}\xi + \zeta + 1)\xi, 0, \xi + \zeta)$ in time $t_3 - t_1 = 2(\frac{1}{2}\xi + \zeta + 1)\xi$. The last sector is a rotation to $(0, (\frac{1}{2}\xi + \zeta + 1)\xi, \xi + \zeta)$ in time $t_4 - t_3 = (\frac{1}{2}\xi + \zeta + 1)\xi$.

Thus the overall map on $\{x_1 = 0 < x_2\}$ is

$$\begin{array}{rcl} \xi_n &=& (1 + \zeta_{n-1} + \frac{1}{2}\xi_{n-1})\xi_{n-1} \ , \\ \zeta_n &=& \zeta_{n-1} + \xi_{n-1} \ , \end{array} \qquad (52)$$

which has an invariant

$$\xi_n - \tfrac{1}{2}\zeta_n^2 = \xi_{n-1} - \tfrac{1}{2}\zeta_{n-1}^2 = ... = \xi_0 - \tfrac{1}{2}\zeta_0^2 \ ,$$

implying that the map $(\xi_{n-1}, \zeta_{n-1}) \mapsto (\xi_n, \zeta_n)$ on $x_1 = 0$ has trajectories lying on the parabolic contours of the function

$$\psi(\xi, \zeta) = \xi - \tfrac{1}{2}\zeta^2 \ .$$

Therefore an orbit that reaches a point $\xi_n = 0$ does so with $\zeta_n = \sqrt{\zeta_0^2 - 2\xi_0}$, and can do so only if it starts on a curve such that $\zeta_0^2 - 2\xi_0 > 0$.

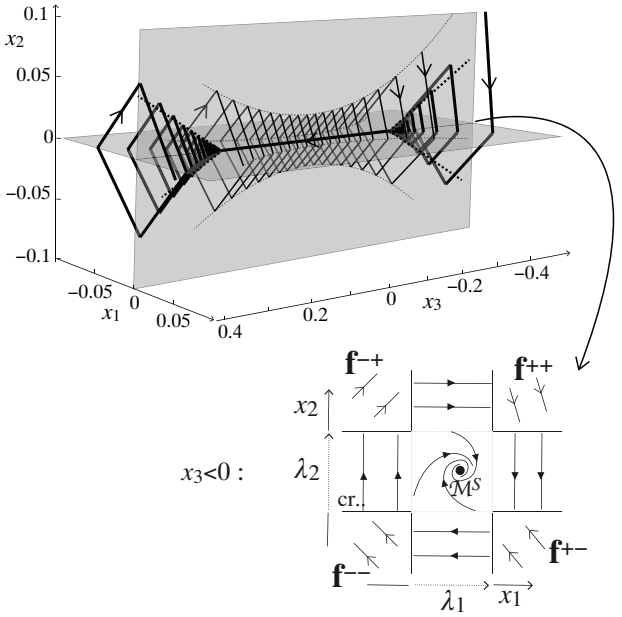

FIG. 16. Sketch of trajectories exhibiting the Zeno phenomenon (bold), taking infinitely many steps in finite time to spiral in towards the intersection in $x_3 < 0$ and out from the intersection in $x_3 > 0$. The inward and outward trajectories are connected by a codimension $r = 2$ sliding trajectory along the intersection. The switching layer system including a sliding manifold $\mathcal{M}^S$ with focal attraction is shown inset (right). A simple trajectory which never reaches the intersection is also shown in the main figure.

While we cannot solve the map, we can easily show that it exhibits the Zeno phenomenon.

Proposition 1. *An orbit starting at* (ξ_0, ζ_0) *such that* $\sqrt{\zeta_0^2 - 2\xi_0} > 0$ *and* $-1 < \zeta_0 < 0$ *converges to* $\xi_n = 0$ *as* $n \to \infty$ *in finite time* $\sqrt{\zeta_0^2 - 2\xi_0} - \zeta_0$.

Proof. An orbit starting at (ξ_0, ζ_0) such that $\sqrt{\zeta_0^2 - 2\xi_0} > 0$ and $-1 < \zeta_0 < 0$ will hit $\xi_n = 0$ when $\zeta_n = \sqrt{\zeta_0^2 - 2\xi_0}$. Since the speed of travel of the flow along the x_3 direction is unity, the time taken is $\Delta T_n = \zeta_n - \zeta_0 = \sqrt{\zeta_0^2 - 2\xi_0} - \zeta_0$, which is clearly finite. We must then show that this orbit takes infinitely many steps, i.e. $\xi_n = 0$ implies $n \to \infty$. Note that $\xi_n = 0$ is a fixed point of the map (52) for any ζ_n. Then by the ξ_n part of (52) we have $\frac{\xi_{n+1}}{\xi_n} = 1 + \zeta_n + \frac{1}{2}\xi_n$, and using the ζ_n part of (52) we can re-write this as $\frac{\xi_{n+1}}{\xi_n} = 1 + \zeta_n + \frac{1}{2}(\zeta_{n+1} - \zeta_n) = 1 + \frac{1}{2}(\zeta_n + \zeta_{n+1})$, which is negative since $\zeta_n, \zeta_{n+1} < 0$. This implies that ξ_n is strictly decreasing towards 0, and therefore cannot terminate at the fixed point 0 in finitely many steps, and thus ξ_n asymptotes towards 0 as $n \to \infty$. □

Conversely, an orbit starting at the intersection in $\zeta_0 > 0$ takes infinitely many steps but finite time to exit from the intersection via the rotation map.

Because an orbit takes infinitely many rotations to reach the intersection, its entry point cannot be determined uniquely, and hence, even if the exit points

from sliding can be determined from the switching layer system, the exit trajectory can also not be determined uniquely, and moreover the exit takes infinitely many steps in finite time.

We conclude with a few simulations of (49). In this case one finds, as predicted, that the exit point along the intersection is very sensitive to numerical imprecision. The simulations shown in figure 17 replace $\lambda_i = \text{sign}\, x_i$ with $\phi(x_i/\varepsilon) = \tanh(x_i/\varepsilon)$ for $i = 1, 2$, with (i) $\varepsilon = 10^{-4}$, (i) $\varepsilon = 10^{-3}$, (i) $\varepsilon = 10^{-2}$. Here the value of the smoothing stiffness ε is more evident, determining how narrow (order ε) the funnelling along the intersection is, but the results are consistent as the exit points occur at similar coordinates $x_3 \approx 0.2$.

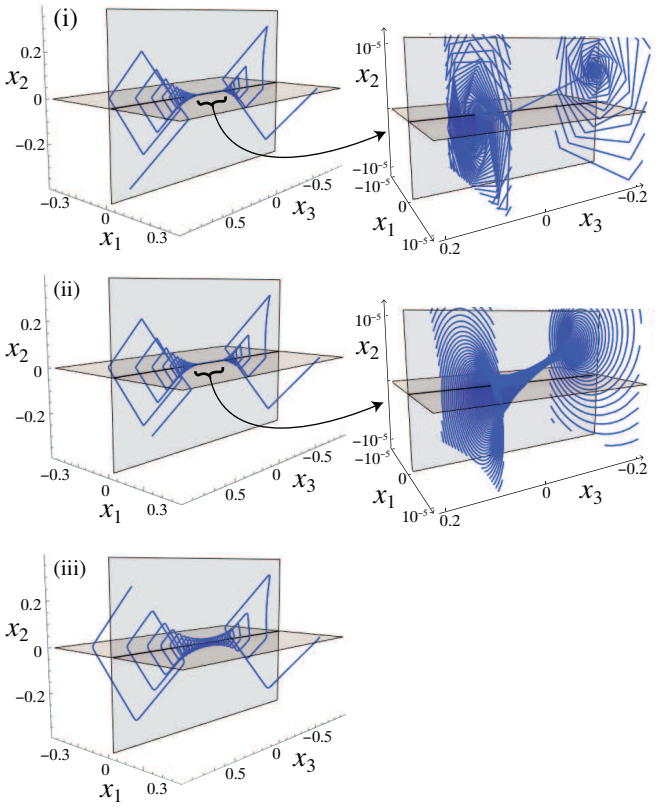

FIG. 17. Simulations using a tanh smoothing with ε values (i) 10^{-4}, (ii) 10^{-3}, (iii) 10^{-2}. For (i)-(ii) a magnification is shown of the funnel along the intersection.

The consistency of these results is further verified by using different smoothings of the sign function, taking the smooth rational function $\phi(x_i/\varepsilon) = (x_i/\varepsilon)/\sqrt{1+(x_i/\varepsilon)^2}$, or the continuous ramp function with $\phi(x_i/\varepsilon) = \text{sign}(x_i)$ for $|x_i| > \varepsilon$ and $\phi(x_i/\varepsilon) = x_i/\varepsilon$ for $|x_i| \leq \varepsilon$. The results for these rational and ramp smoothings are qualitatively indistinguishable from the tanh smoothing, though with some difference in the thickness of the funnel visible for $\varepsilon = 10^{-3}$, but with similar exit points around $x_3 \approx 0.2$.

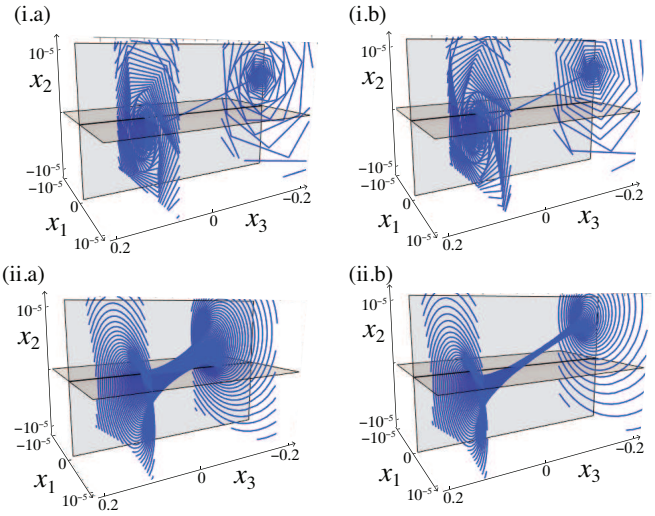

FIG. 18. The attractors in figure 17(i-ii) for the rational (a) and ramp (b) smoothings, with the same initial conditions, for $\varepsilon = 10^{-3}$.

V. EXAMPLE OF COUPLED OSCILLATORS

We have so-far looked at single or double tangencies to a codimension $r = 2$ switching surface, as the basic mechanisms for exit from sliding. In systems of many dimensions with many switches, such as those suggested in (2)-(4), many such exits may occur, taking a similar form from higher codimension intersections. Moreover, because a system with n dimensions and a switching surface comprised of r transverse manifolds may generically exhibit exit points consisting of up to $n-r$ tangencies on independent switching surfaces, these events may tend to cluster, and form exit cascades. Those cascades arise quite easily observed in models like (2)-(4), as we show here.

Take an example of an oscillator system similar to those in the introduction, specifically

$$\left.\begin{aligned} \dot{z}_i &= y_i \,, \\ \dot{y}_i &= -M^{\rho}_{ij} y_j - M^{\kappa}_{ij} z_j - \mu\,(y_i - v) \,, \end{aligned}\right\} \quad i = 1, ..., n/2,$$

where M^{ρ} and M^{κ} are matrices, and n is an even integer. The matrix of damping coefficients is diagonal with components in the range $M^{\rho}_{ij} \in [\rho, 2\rho]$, the matrix of spring coefficients has an antisymmetric part and a diagonal part with components in the range $M^{\kappa}_{ij} \in [-\kappa, +\kappa]$. The model represents a network of oscillators with displacements x_i and velocities y_i, connected via spring-damper couplings, and with every oscillator also having a strength coupling to some parent object. The couplings are generated randomly, therefore M^{ρ} and M^{κ} are random matrices (up to symmetries). The parent slips at a constant speed v, and each oscillator experiences a dry (Coulomb) friction force against the surface with friction coefficient unity. The system is non-conservative due to the linear and frictional damping and the energy input

from the slipping surface.

Let $x_{2i-1} = z_i$, $x_{2i} = y_i$. We have $n/2$ switching surfaces $h_i = y_i - v = 0$. A trajectory crosses a switching surface transversally when an oscillator in the system alternates between left and right slipping motion. A trajectory slides on a codimension r switching surface intersection when r oscillators experience frictional sticking, so that their speeds are each fixed $y_i = v$.

In simulations the oscillators typically exhibit either collapse to a low codimension sliding (where most oscillators are slipping) or else exhibit complex transitions between higher and lower codimension sliding, indicating many oscillators sticking and releasing in complex patterns: when one oscillator slips it may trigger an avalanche of many slips events across different oscillators or not. Decreases in the sliding codimension r take place via exit points as described above.

Visualizing the dynamics directly becomes, of course, impossible, however the simulations in figure 19, showing just three of the 400 dimensions, do give a fair representation of the dynamics. Two cases are shown, one in which the system exhibits sustained complex oscillations which continually attach and exit from the switching manifolds (left), and one in which all sliding ceases and the system escapes, meaning that blocks change direction without sticking and increasingly grow in speed.

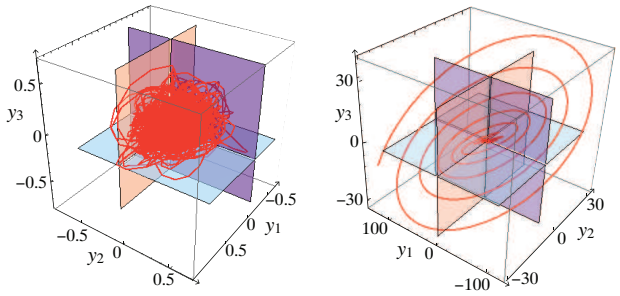

FIG. 19. Oscillator simulations for (iii) and (iv) from figure 20.

To view this dynamics usefully we can use the sliding codimension r. Drops in the value of r correspond to exit points. Figure 20 shows values of r calculated from simulations along a trajectory over large times, for: (i) 100 oscillators, $v = -0.45$, $\varepsilon = 0.03$, $\rho = 3$, $\kappa = 0.2$; (ii) 200 oscillators, $v = -0.2$, $\rho = 3.5$, $\kappa = 0.2$; (iii) 200 oscillators, $v = -0.2$, $\rho = 3.5$, $\kappa = 0.22$; (iv) 200 oscillators, $v = -0.3$, $\rho = 3.5$, $\kappa = 0.3$. We model the switch as $\text{sign}u = \tanh(u/\varepsilon)$ with $\varepsilon = 0.03$ (and simulations not show qualitative dependence on ε). In (i)-(iii), the system exhibits sustained and complex oscillatory dynamics, with erratic increases and decreases in r, all, however, tending to vary around an approximate value of $\sqrt{n/2}$. In (iv) the oscillations eventually die away and all blocks escape from sliding.

A continual decrease in r corresponds to a cascade of exit events (stick-to-slip events in mechanical terms). The frequency of cascades of size r is plotted in figure 21 for each of the simulations in figure 20, revealing a log-

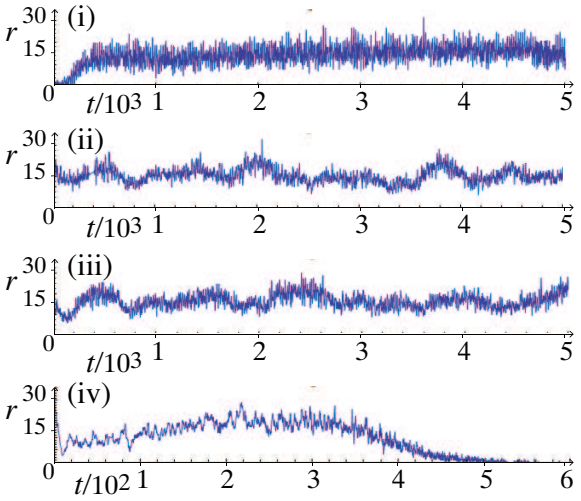

FIG. 20. Stick-slip events as measured by sliding codimension r.

arithmic distribution. Note that the power law is exhibited regardless of whether the system remains in highly critical state or suffers complete eventual collapse. Ongoing work is examining the particular exit points and their roles in generating such avalanches.

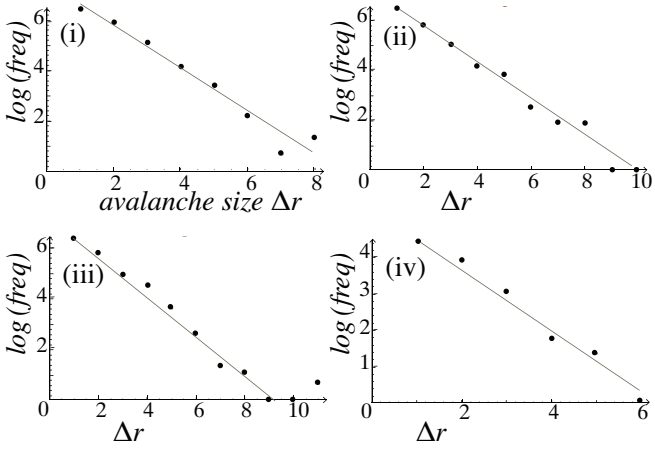

FIG. 21. Plot of frequency of cascade events by size. A cascade is a sequence of drops in sliding codimension r, the size being the overall decrease in r. The gradients are -0.86, -0.70, -0.82, -0.89 (for fitting we disregard the last two data points).

VI. CLOSING REMARKS

We are only at the beginning of the study of exit points. Rather than begin a classification that would be limited to low dimensions, we have focussed on dynamical phenomena such as exit points and determinacy-breaking, which form the basis for behaviour in higher dimensions and which might have distinct implications for applications. Particularly interesting is the collapse to higher

order sliding that forms highly critical states, and the subsequent large scale reorganization through avalanches of exit points which, at least in the example studied here, satisfy power law size-frequency distributions.

We have analysed the basic mechanisms by which determinacy-breaking affects a piecewise smooth flow with one or two switches. The flow outside the switching surface suggests that determinacy fails at certain points where the flow is transversal to the switching thresholds. Whereas each initial condition has a unique forward time orbit almost everywhere in the flow, at the intersection the flow becomes set-valued. A switching layer analysis of the intersection is required to reveal what is happening in more detail, restoring determinacy to some extent, but revealing sensitivity to initial conditions and a dependence on parameters, which is not evident if we neglect the 'hidden dynamics' inside the switching surfaces.

Several of the cases studed here can be analyzed in more detail, but we have focussed on bringing out their common features, and demonstrating the methods that can be used to study them. To develop a systematic classification remains an open problem, and it is to be hoped that results such as that concerning equation (48) in section IV A, showing that a double codimension $r = 1$ sliding tangency to a codimension $r = 2$ intersection has the same local form as the two-fold (a double codimension $r = 0$ vector field tangency to a codimension $r = 1$ switching manifold), can be generalized. Particularly interesting for future work is to study points where there are tangencies of multiple codimension $r-1$ sliding flows to a codimension r intersection, generalizing the $r = 1$ and $r = 2$ cases studied here.

[1] M. A. Aizerman and E. S. Pyatnitskii. Fundamentals of the theory of discontinuous systems I,II. *Automation and Remote Control*, 35:1066–79, 1242–92, 1974.

[2] J. Awrejcewicz, L. Dzyubak, and C. Grebogi. Estimation of chaotic and regular (stick-slip and slip-slip) oscillations exhibited by coupled oscillators with dry friction. *Nonlinear Dynamics*, 42:383–394, 2005.

[3] G. Bachar, E. Segev, O. Shtempluck, E. Buks, and S. W. Shaw. Noise induced intermittency in a superconducting microwave resonator. *EPL*, 89(1):17003, 2010.

[4] G-I. Bischi, F. Lamantia, and D. Radi. Multispecies exploitation with evolutionary switching of harvesting strategies. *Natural Resource Modeling*, 26(4):546–571, 2013.

[5] R. Burridge and L. Knopoff. Model and theoretical seismicity. *Bull. Seism. Soc. Am.*, 57:341–371, 1967.

[6] A. Colombo, M. di Bernardo, S. J. Hogan, and M. R. Jeffrey. Bifurcations of piecewise smooth flows: perspectives, methodologies and open problems. *Physica D: Special Issue on Dynamics and Bifurcations of Nonsmooth Dynamical Systems*, 241(22):1845–1860, 2012.

[7] A. Colombo and M. R. Jeffrey. The two-fold singularity: leading order dynamics in n-dimensions. *Physica D*, 265:1–10, 2013.

[8] M. Desroches, B. Krauskopf, and H. M. Osinga. Numerical continuation of canard orbits in slow-fast dynamical systems. *Nonlinearity*, 23(3):739–765, 2010.

[9] M. di Bernardo, C. J. Budd, A. R. Champneys, and P. Kowalczyk. *Piecewise-Smooth Dynamical Systems: Theory and Applications*. Springer, 2008.

[10] M. di Bernardo, P. Kowalczyk, and A. Nordmark. Sliding bifurcations: a novel mechanism for the sudden onset of chaos in dry friction oscillators. *Int.J.Bif.Chaos*, 10:2935–2948, 2003.

[11] L. Dieci. Sliding motion on the intersection of two surfaces: spirally attractive case. *submitted Aug. 2014*, 2014.

[12] L. Dieci, C. Elia, and L. Lopez. A Filippov sliding vector field on an attracting co-dimension 2 discontinuity surface, and a limited loss-of-attractivity analysis. *J. Differential Equations*, 254:1800–1832, 2013.

[13] A. F. Filippov. *Differential Equations with Discontinuous Righthand Sides*. Kluwer Academic Publ. Dortrecht, 1988 (Russian 1985).

[14] M. R. Francis and E. J. Fertig. Quantifying the dynamics of coupled networks of switches and oscillators. *PLOSOne*, 7(1):1–8, 2012.

[15] P. Glendinning and M. R. Jeffrey. Grazing-sliding bifurcations, the border collision normal form, and the curse of dimensionality for nonsmooth bifurcation theory. *Nonlinearity*, 28:263–283, 2014.

[16] A. V. Hill. The possible effects of the aggregation of the molecules of haemoglobin on its dissociation curves. *Proc. Physiol. Soc.*, 40:iv–vii, 1910.

[17] S. J. Hogan, M. E. Homer, M. R. Jeffrey, and R. Szalai. Piecewise smooth dynamical systems theory: the case of the missing boundary equilibrium bifurcations. *submitted*, 2015.

[18] M. R. Jeffrey. Dynamics at a switching intersection: hierarchy, isonomy, and multiple-sliding. *SIADS*, 13(3):1082–1105, 2014.

[19] M. R. Jeffrey. Hidden dynamics in models of discontinuity and switching. *Physica D*, 273-274:34–45, 2014.

[20] M. R. Jeffrey. Fold singularities of nonsmooth and slow-fast dynamical systems – equivalence through regularization. *submitted*, 2015.

[21] Yu. A. Kuznetsov, S. Rinaldi, and A. Gragnani. One-parameter bifurcations in planar Filippov systems. *Int. J. Bif. Chaos*, 13:2157–2188, 2003.

[22] D. N. Novaes and M. R. Jeffrey. Regularization of hidden dynamics in piecewise smooth flow. *J. Differ. Equ.*, 259:4615–4633, 2015.

[23] S. H. Piltz, M. A. Porter, and P. K. Maini. Prey switching with a linear preference trade-off. *SIAM J. Appl. Math.*, 13(2):658–682, 2014.

[24] E. Plahte and S. Kloglum. Analysis and generic properties of gene regulatory networks with graded response functions. *Physica D*, 201:150–176, 2005.

[25] D. J. W. Simpson. Scaling laws for large numbers of coexisting attracting periodic solutions in the border-collision normal form. *Int. J. Bif. Chaos*, 24(9):1–28, 2014.

[26] M. A. Teixeira. Generic bifurcation of sliding vector fields. *J. Math. Anal. Appl.*, 176:436–457, 1993.

[27] M. A. Teixeira and P. R. da Silva. Regularization and singular perturbation techniques for non-smooth systems.

Physica D, 241(22):1948–55, 2012.

[28] V. I. Utkin. Variable structure systems with sliding modes. *IEEE Trans. Automat. Contr.*, 22, 1977.

[29] V. I. Utkin. *Sliding modes in control and optimization.* Springer-Verlag, 1992.

[30] M. Wechselberger. Existence and bifurcation of canards in $\mathbb{R}^3$ in the case of a folded node. *SIAM J. App. Dyn. Sys.*, 4(1):101–139, 2005.